Resuspension of Flooded Mine Tailings

Ernest K. Yanful

The UNIVERSITY of WESTERN ONTARIO

LONDON, ONTARIO, CANADA, N6A 5B9

Acknowledgements

- NSERC
- Mining Industry (Falconbridge, Noranda, Rio Algom, Inco, Teck, Cambior, and Newmont Canada)
- 7 graduate students and 1 Postdoctoral Fellow at Western
- 5 Research Collaborators (Profs at Western)

Water cover

- Wind
- Current
- Waves
- Tailings
- Water depth
- Critical shear stress

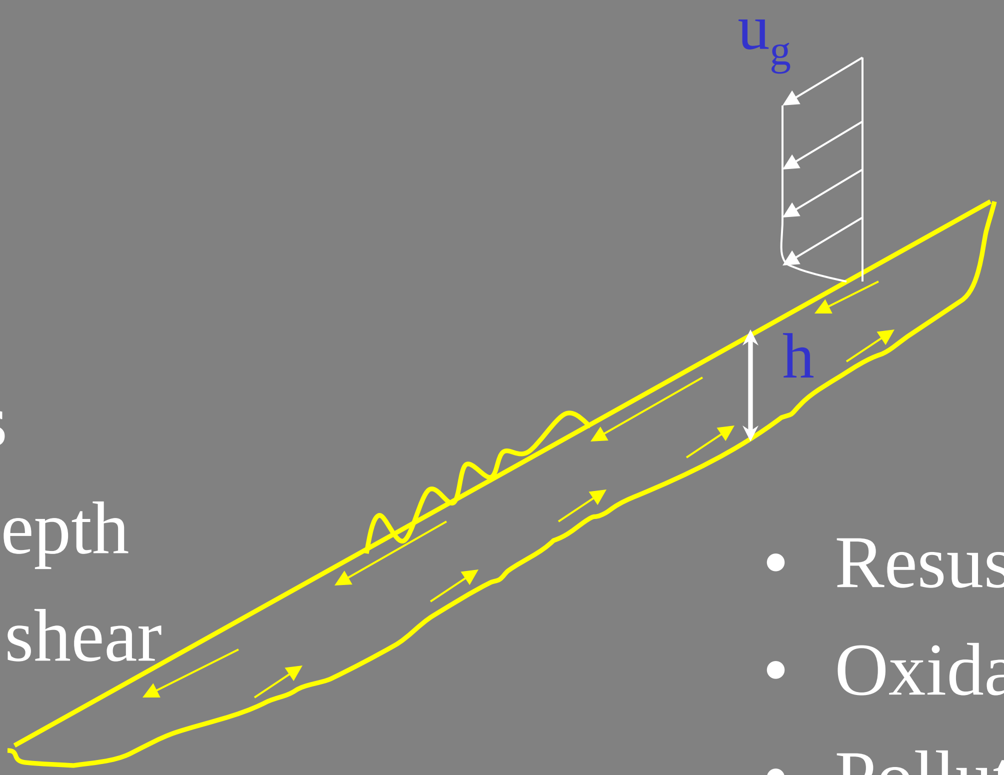

- Resuspension
- Oxidation
- Pollution

Schematic of Conceptual Tailings Pond Hydrodynamics

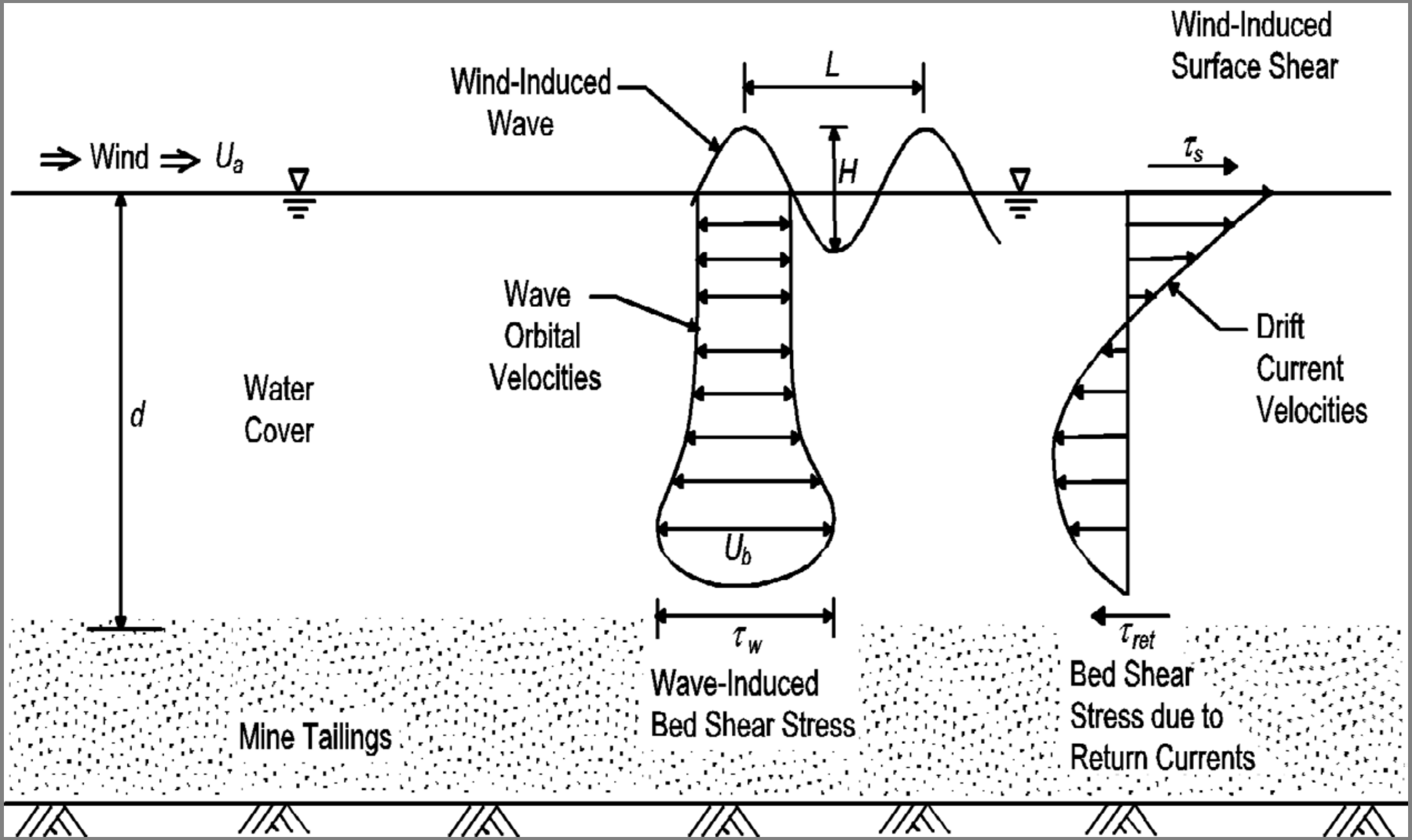

Flow field visualization
for wind speed u_g=6.39m/s and water depth h=63.5 mm
(Deep water wave)

Wind

Surface drift

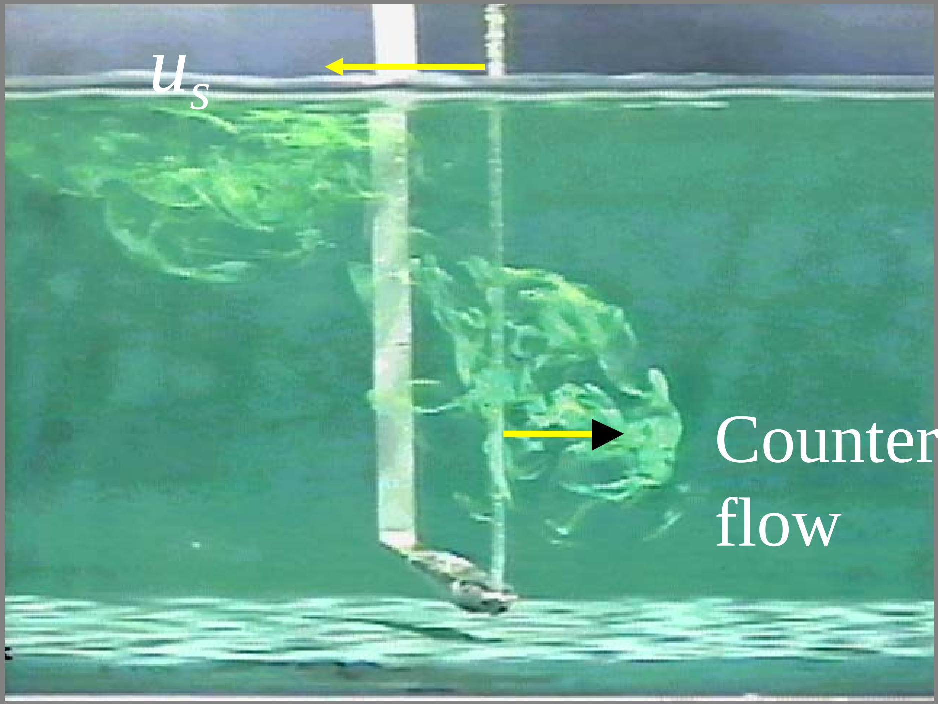

Study of surface **shear** and **waves** induced countercurrent flow

- Experimental Study
- Mathematical modeling

Classification of waves

- **Deep: h/λ>1/2**
- **Intermediate: 1/20<h/λ<1/2**
- **Shallow: h/λ<1/20**

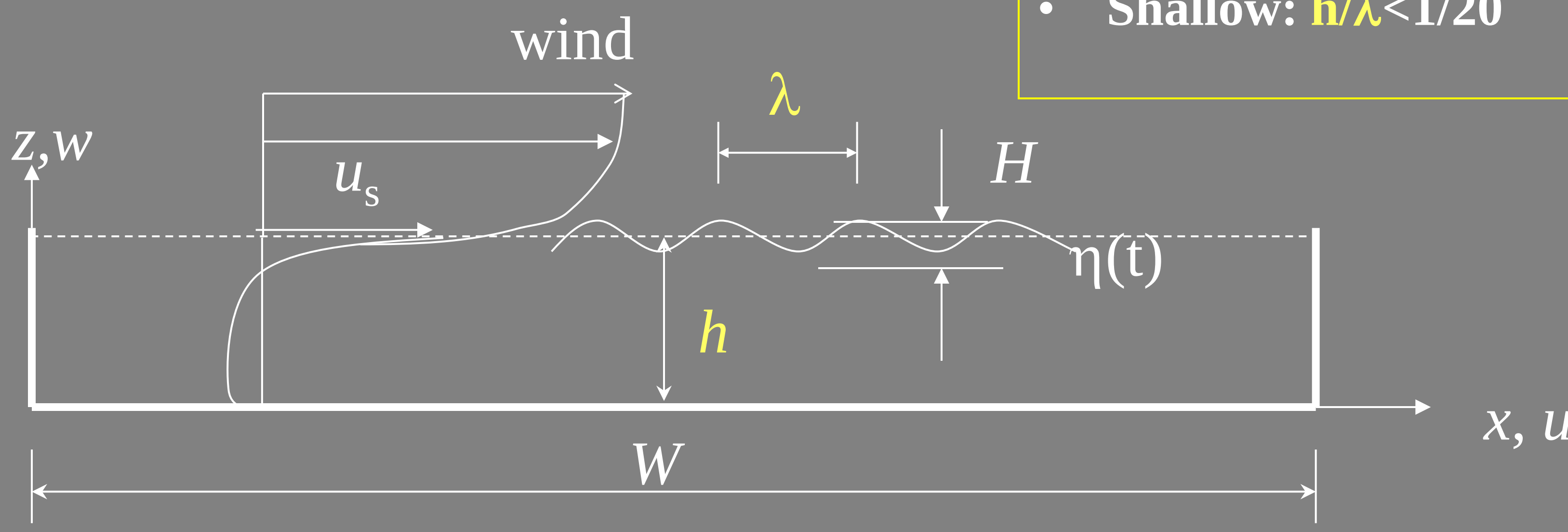

Field Resuspension Studies

- Field Studies
  - Heath Steele Upper and Lower Cells near Miramichi, New Brunswick
  - Quirke Cell 14, near Elliot Lake, Ontario
  - Falconbridge New Tailings Area, Near Sudbury, Ontario
- Laboratory Studies
  - Wave Tank and Wind-Wave Tank Experiments


Heath Steele
QUEBEC
MAINE
UNITED STATES
PRINCE EDWARD ISLAND
NOVA SCOTIA
Gulf of St. Lawrence
Bay of Fundy
Confederation Bridge
Dalhousie
Campbellton
Pointe-Verte
Miscou Centre
Caraquet
Petit Rocher
Beresford
Shippegan
Kedgwick
Bathurst
Tracadie
Sheila
Allardville
Brantville
St. Quentin
Edmundston
Saint-Basile
Neguac
Laviliette
Saint-Léonard
Drummond
Grand Falls
Newcastle
Chatham
Baie-Sainte-Anne
Plaster Rock
Nelson-Miramichi
Perth-Andover
Rogersville
Richibucto
Juniper
Doaktown
Bouctouche
Bristol
Astle
Harcourt
Stanley
Shediac
Cap-Pelé
Woodstock
Moncton
Dieppe
Riverview
Memramcook
Nackawic
Fredericton
Dorchester
Sackville
Oromocto
Sussex
Norton
Tracy
Alma
McAdam
Quispamsis
Hampton
Grand Bay
Fairvale
St. Martins
St. Stephen
Saint John
St. George
Blacks Harbour
Halifax
0 30 60 mi
0 40 80 km
70° 69° 68° 67° 66° 65° 64° 63°
47° 46° 45°
NEW BRUNSWICK
CITIES
Political subdivision capitals
Cities
BOUNDARIES
International
Political subdivision
©1999, Encyclopædia Britannica, Inc.

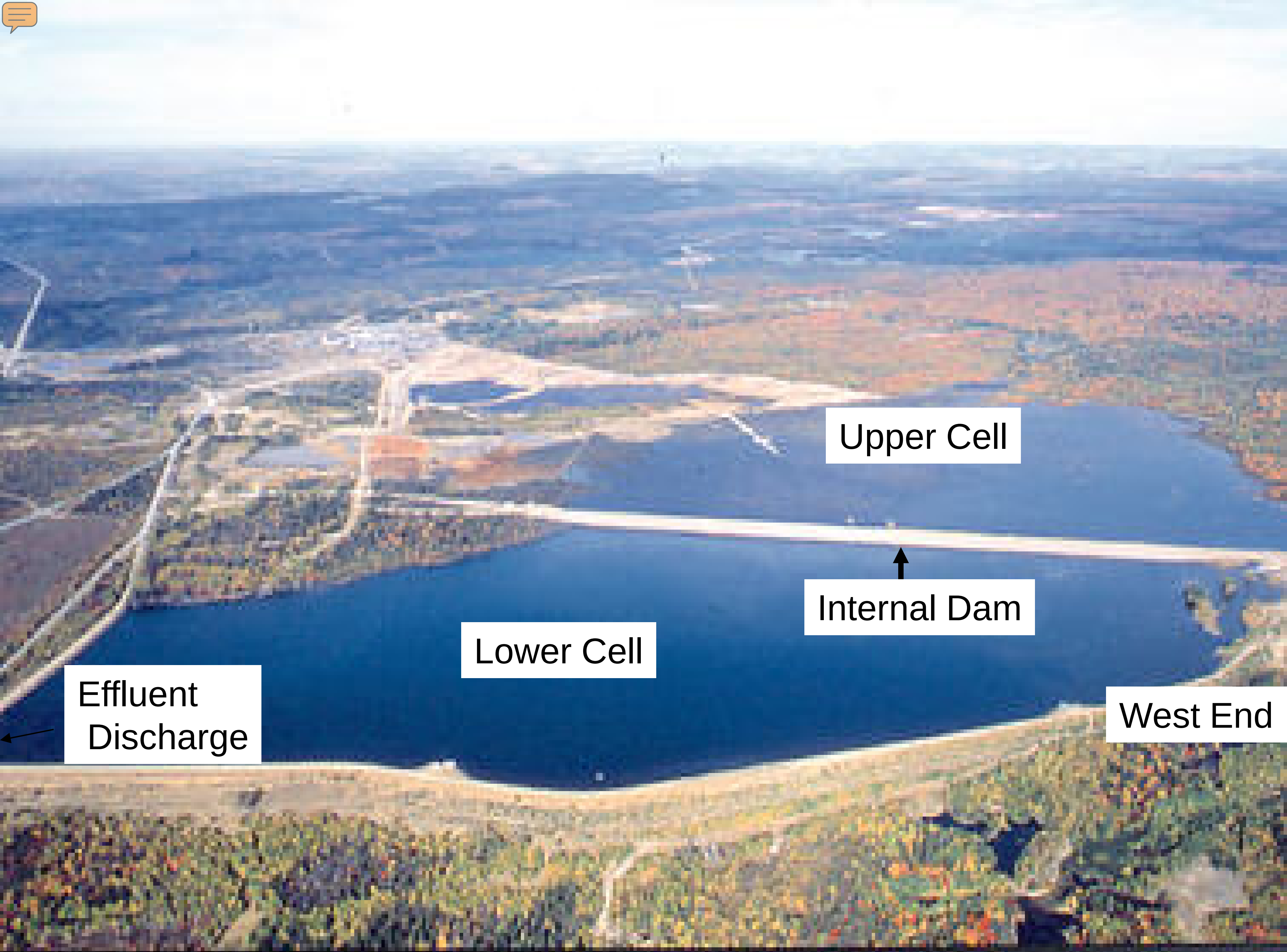
Upper Cell
Internal Dam
Lower Cell
Effluent Discharge
West End

Heath Steele Upper Cell Tailings Pond Showing Sediment Trap Locations

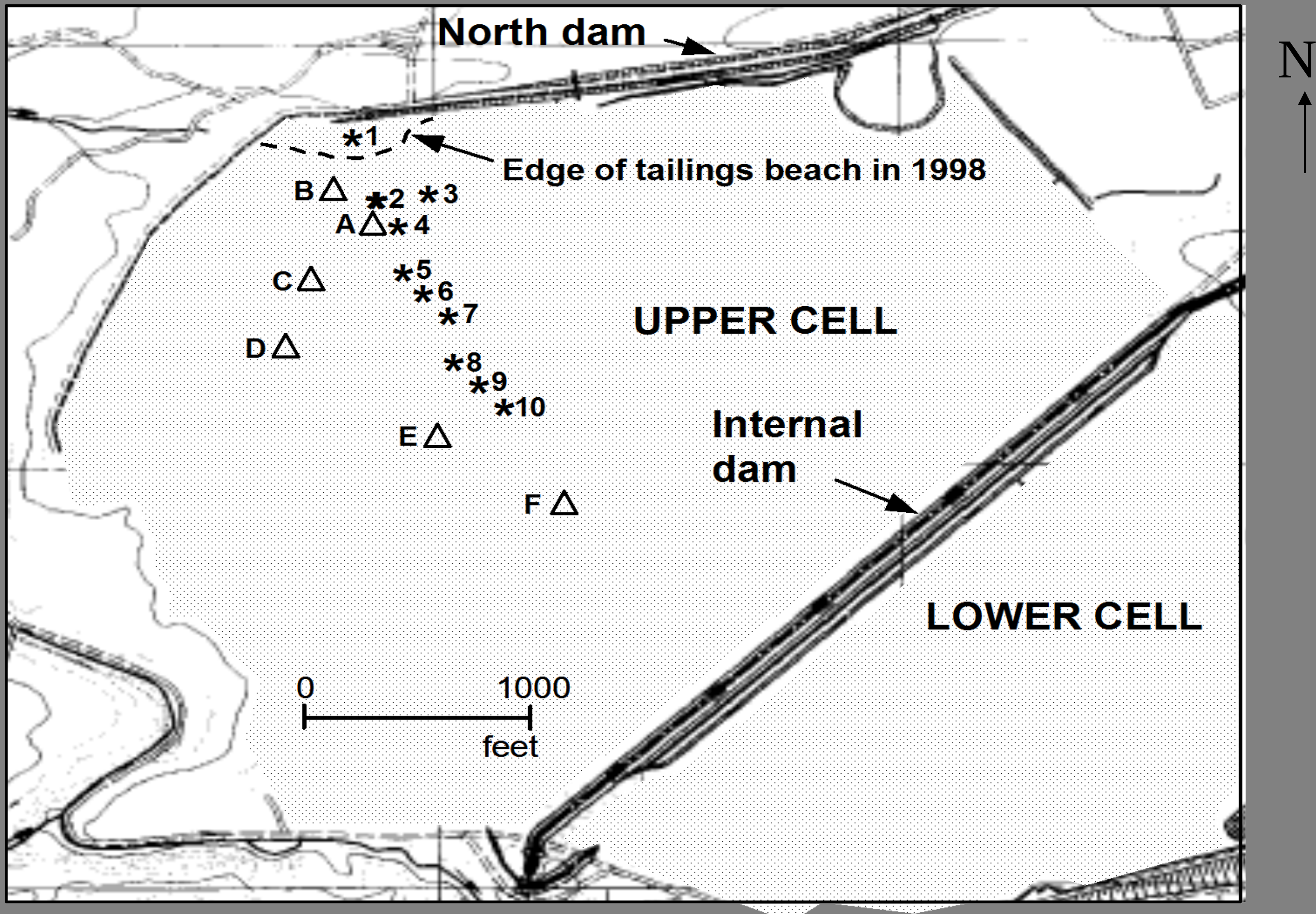

Schematic of sediment trap

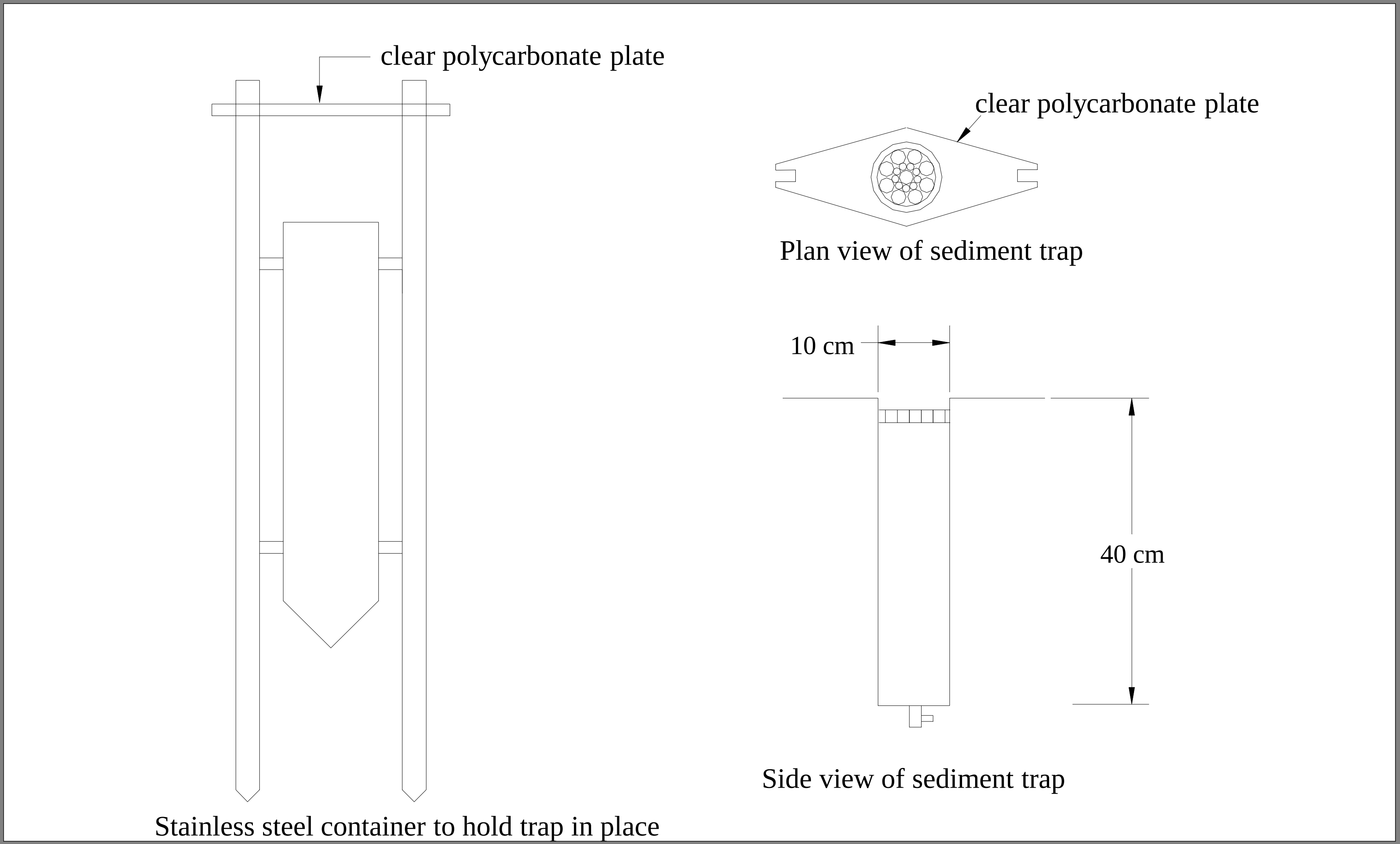

Wind Measurements

- Wind Speed
- Wind Direction

Wave Measurements

- Quirke Cell 14, 0.38 – 1.5 m
- Heath Steele Upper Cell
  0.9 –1.2 m

Time History of Surface Elevation

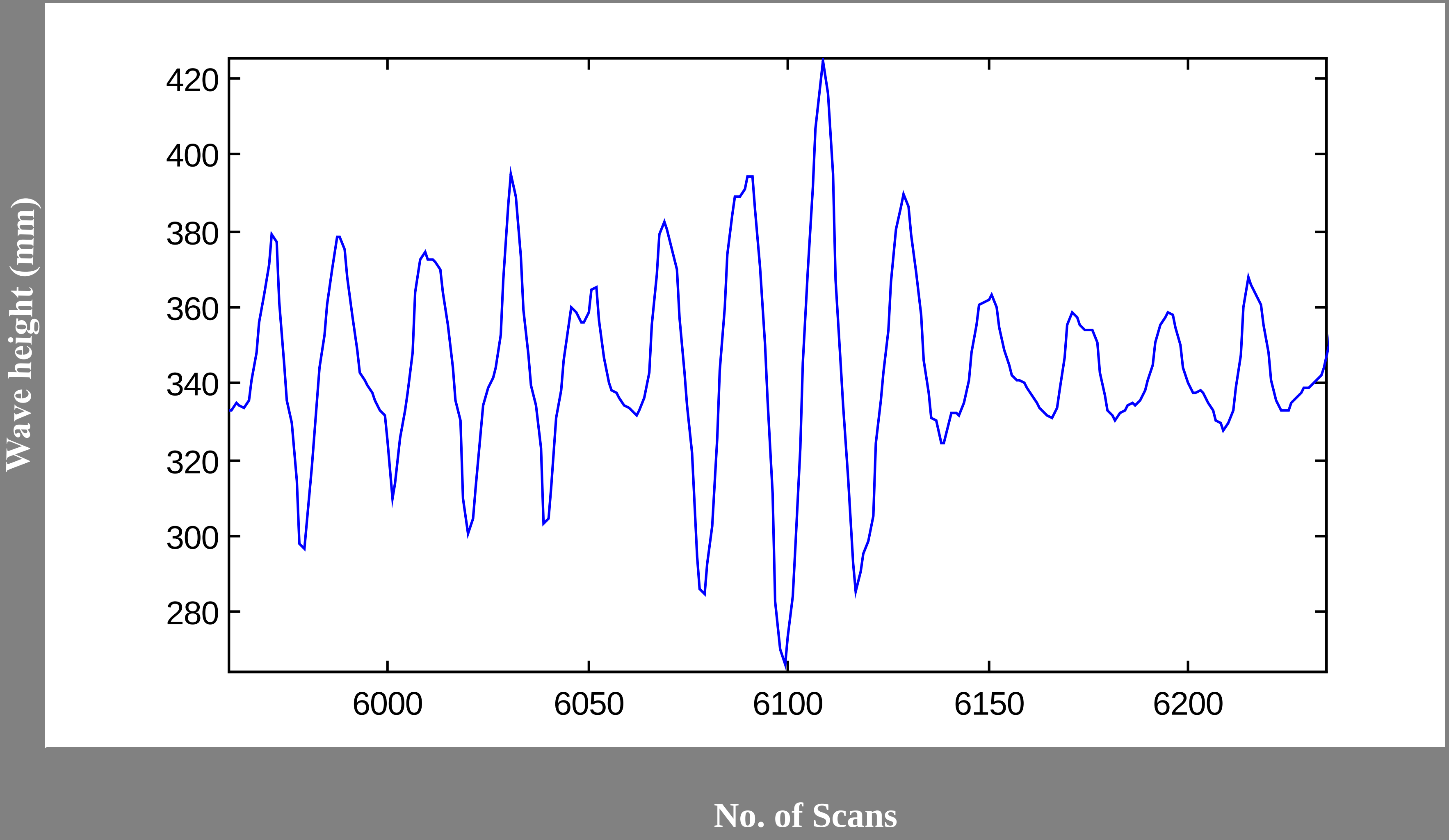

Data Processing

- Spectral analysis (root mean square approach)

$$H_s = 1.416 H_{rms} = 1.416\sqrt{\sum_{i=1}^{N} Hi^2 \Big/ N} \approx 4\sqrt{m_o} = 4\sigma_n$$

  - *Hs* (significant wave height)

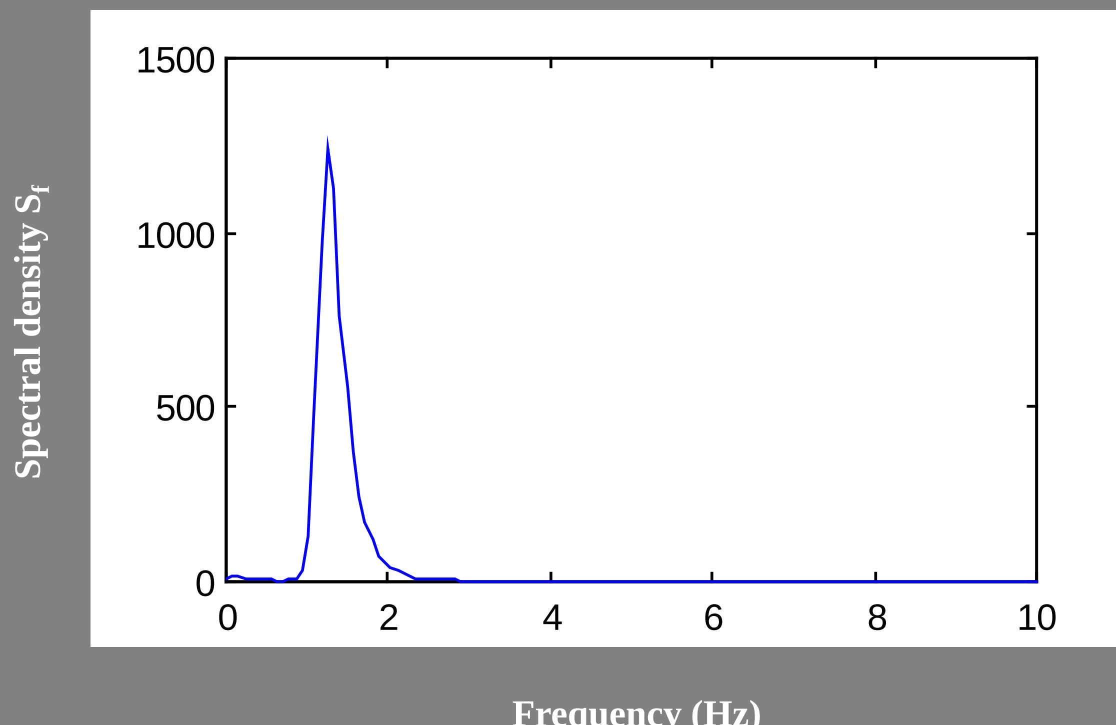

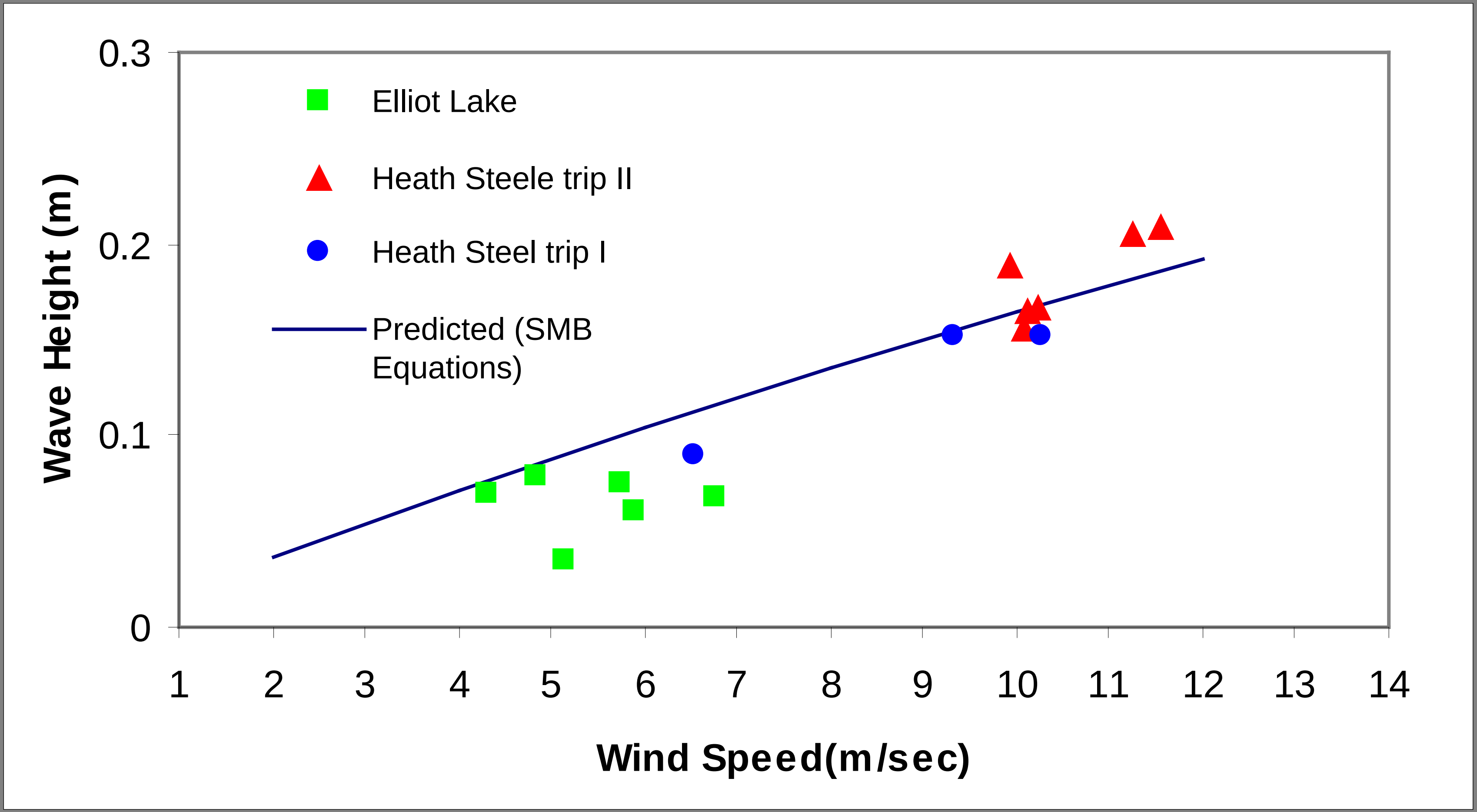

Measured and predicted wave heights for 1 m

Wind Frequency Diagram: Heath Steele

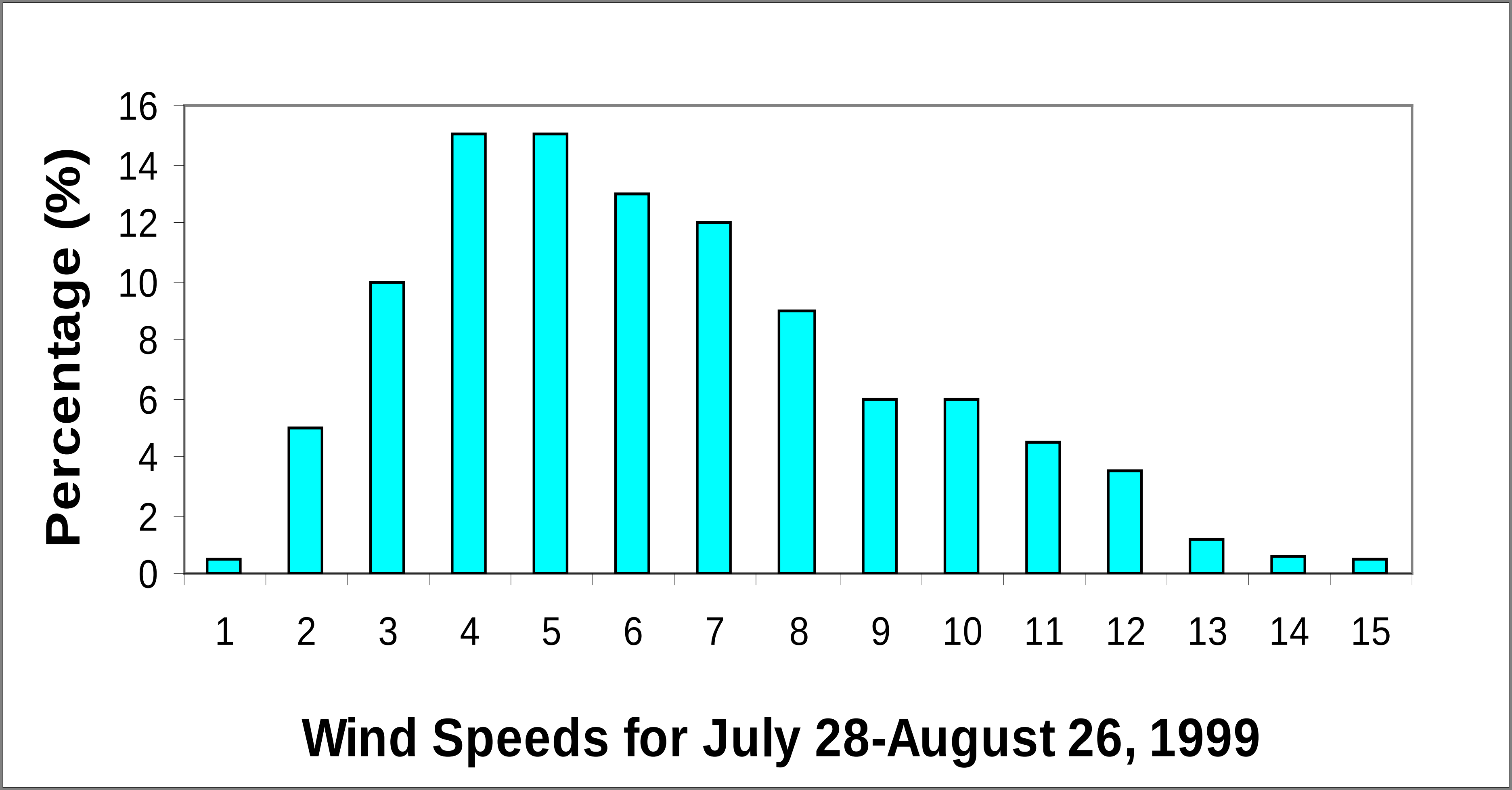

Grain Size Distribution

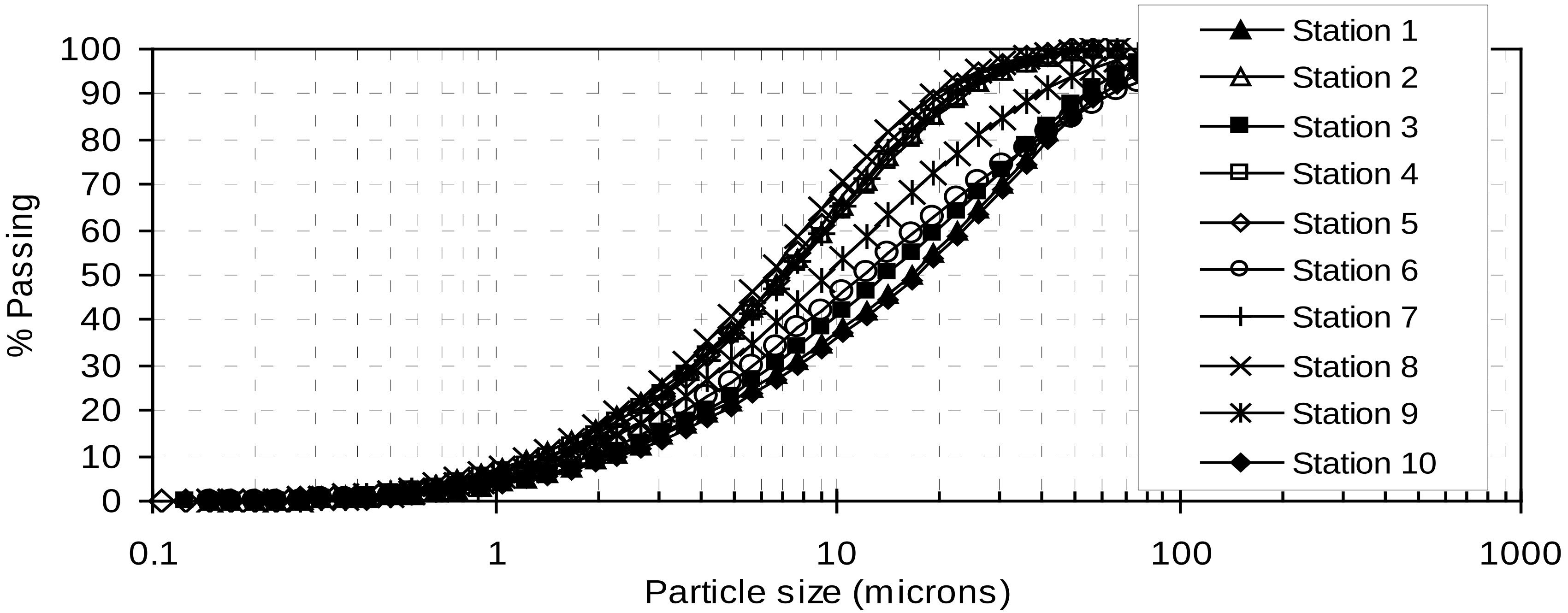

Figure 1 Particle size distributions of bed tailings at different stations (Heath Steele Upper Cell Pond)

Side View of Laboratory Annular Flume and Ring (Modified from Krishnappan, 1993)

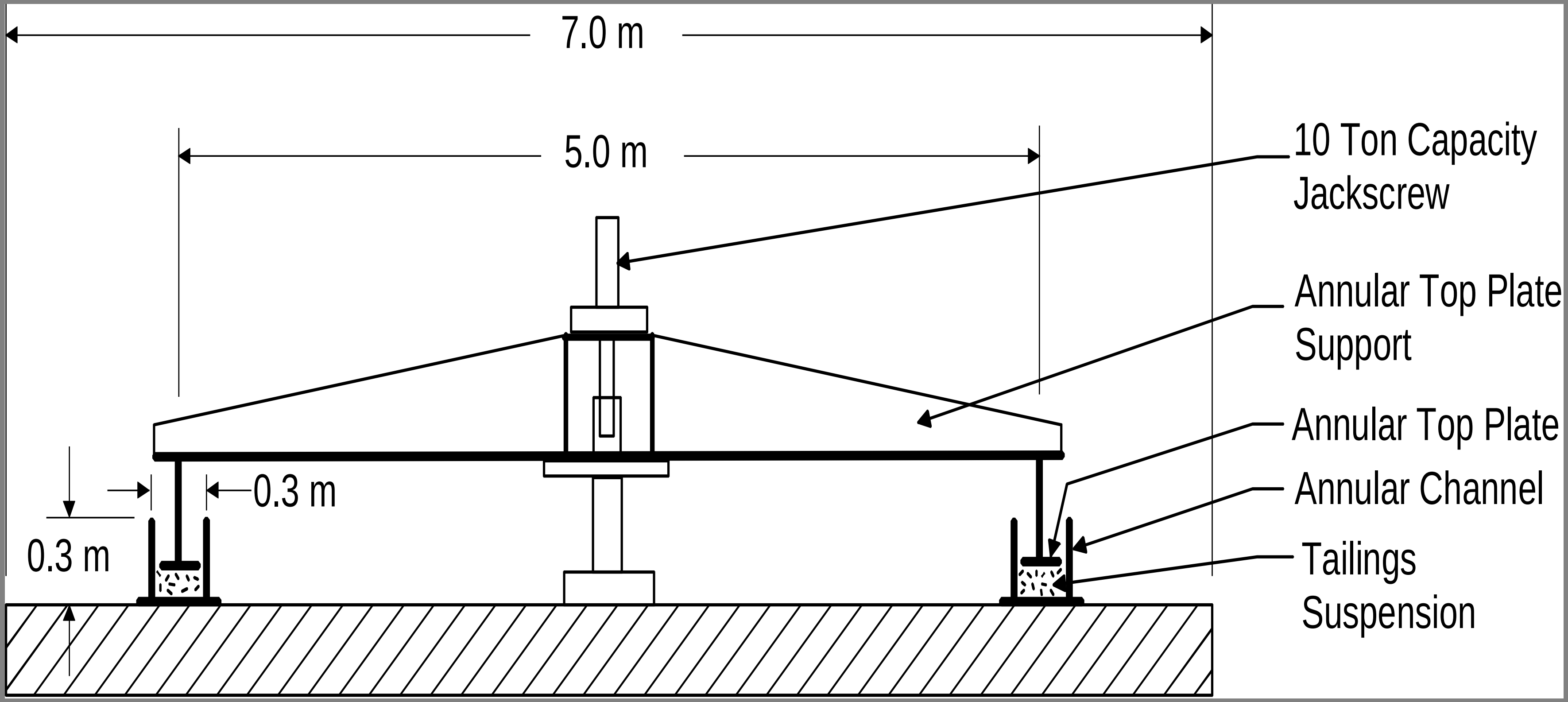

Shear Stress and Suspended Tailings Concentration Measured in Rotating Flume

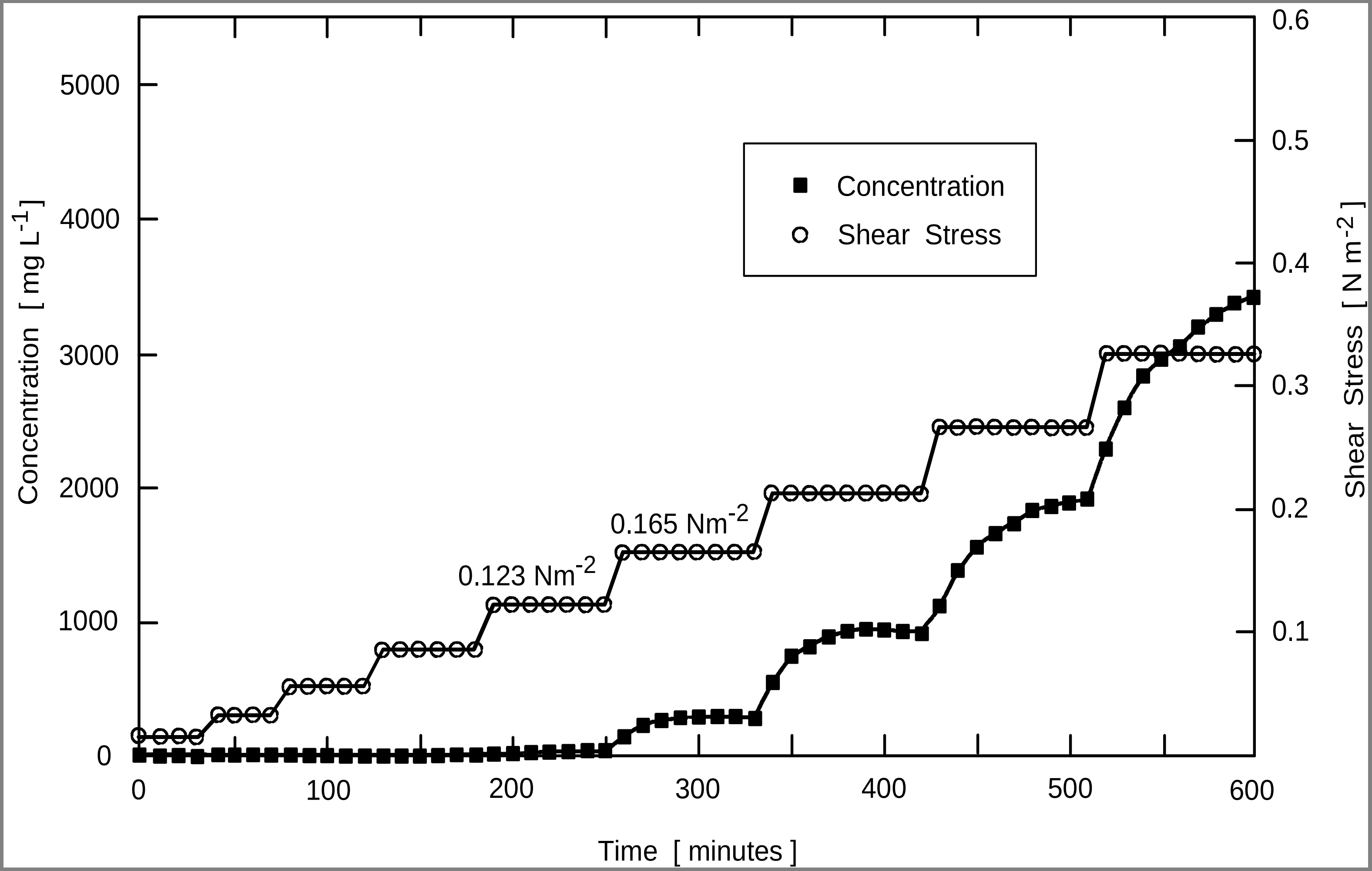

Plots Showing the Transition from Deep Water Wave to Shallow Water Wave Conditions in 0.75 m to 2 m Water Depth

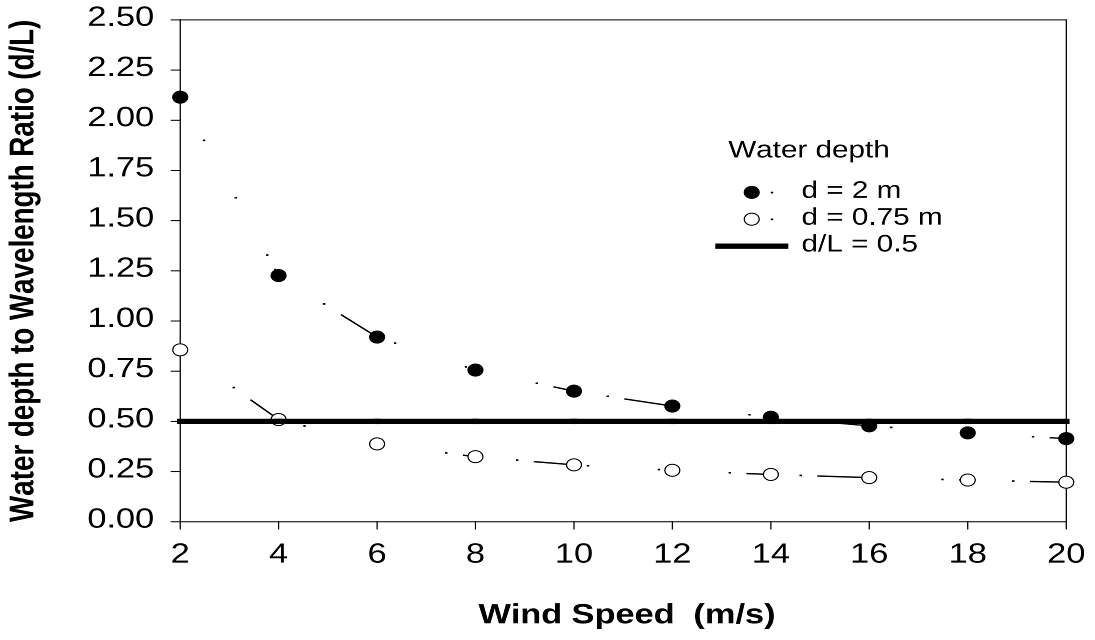

Figure 6 Plots showing transition from deep water wave (d/L >0.5) to shallow water wave (d/L < 0.5) conditions in 0.75 m and 2 m water covers at different wind speeds

Comparison of Predicted Total Bed Shear Stress and Measured Shear Stress of Heath Steele Mine Tailings under 1 m Water Cover

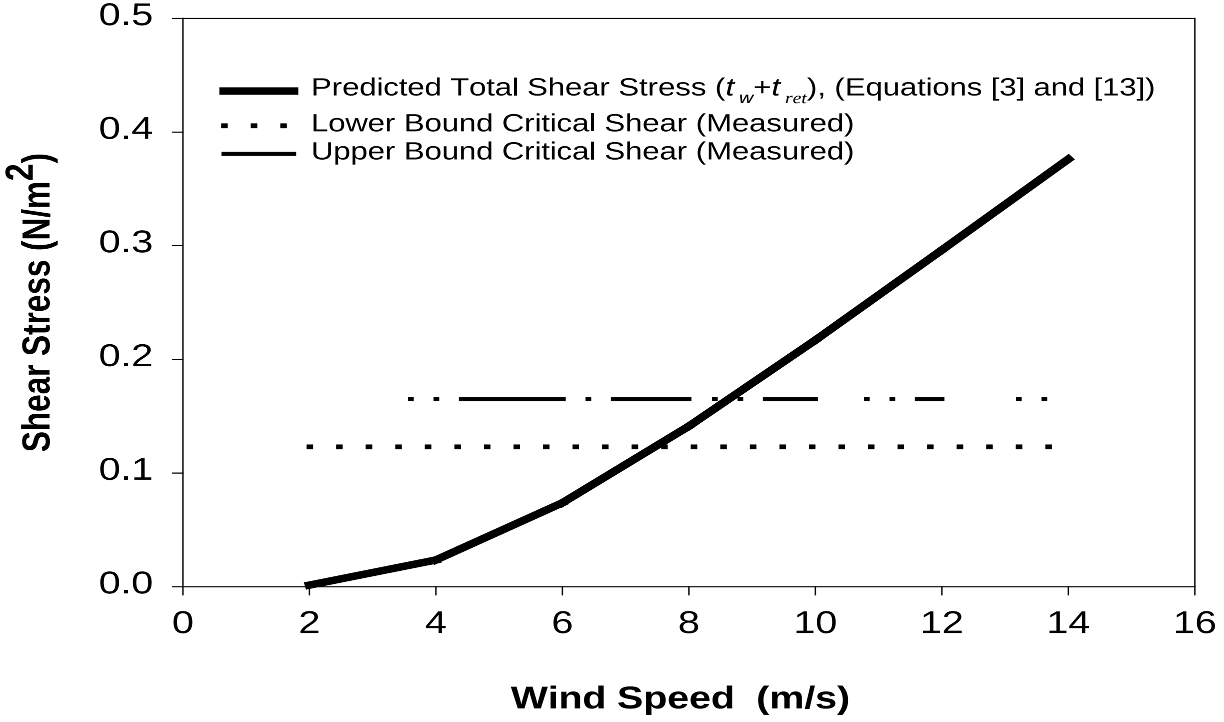

Figure 10 Comparison of predicted total bed shear stress under 1-m water cover and measured critical shear stress of Heath Steele mine tailings

Predicted Critical Wind Speed for Erosion versus Water Cover Depth (Heath Steele)

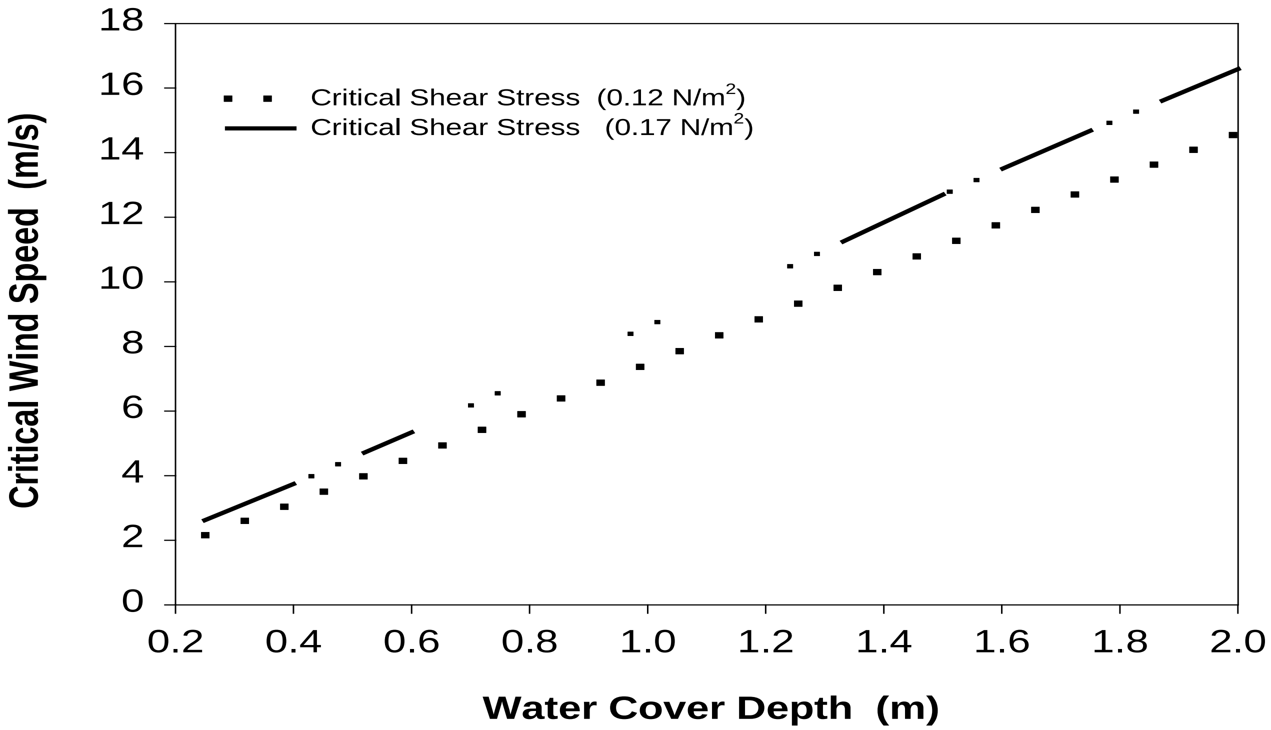

Figure 11 Predicted critical wind speed for erosion versus water cover depth (Heath Steele Mine Upper Cell tailings pond)

Metals as Tracers : Heath Steele Upper Cell

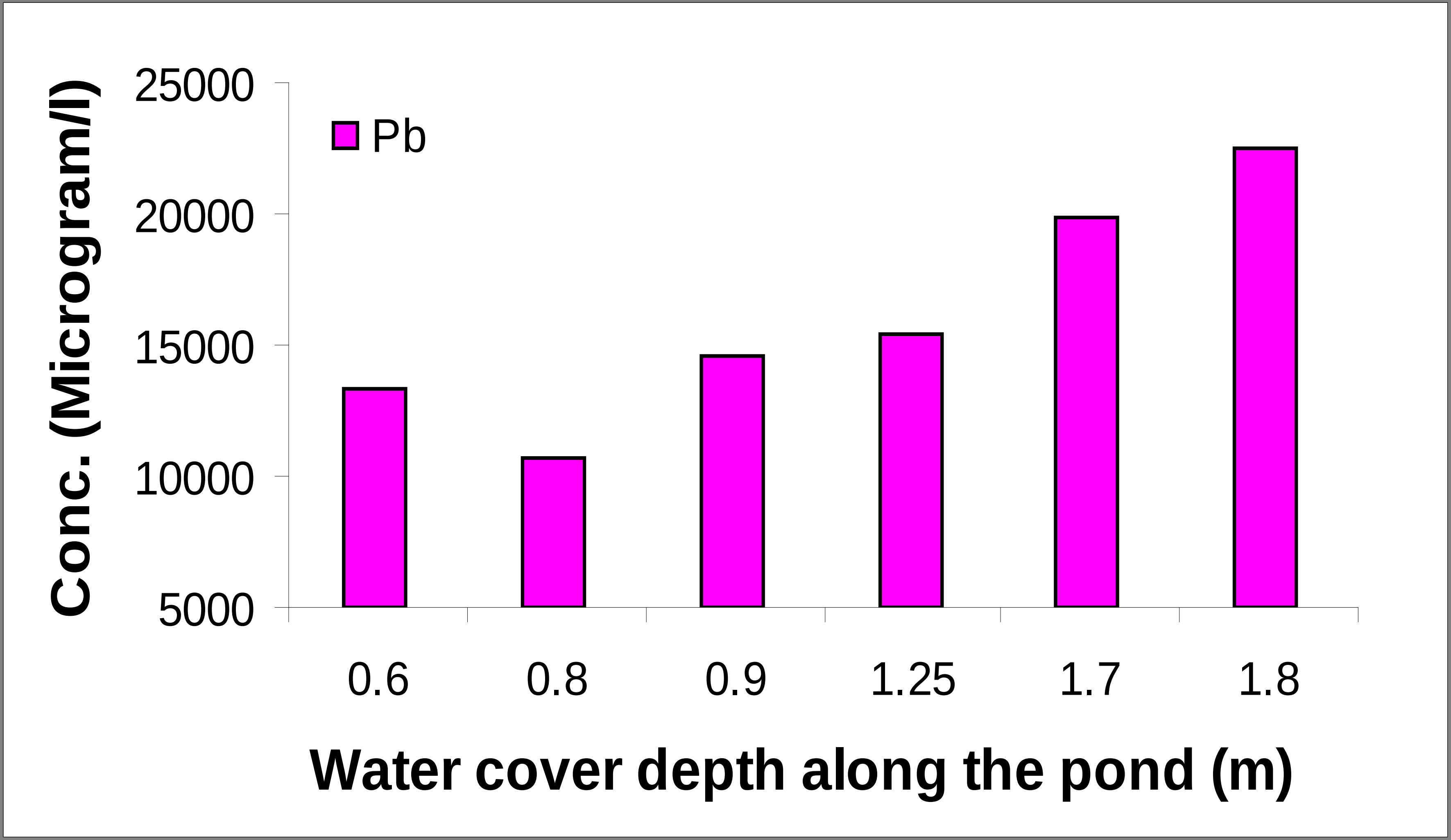

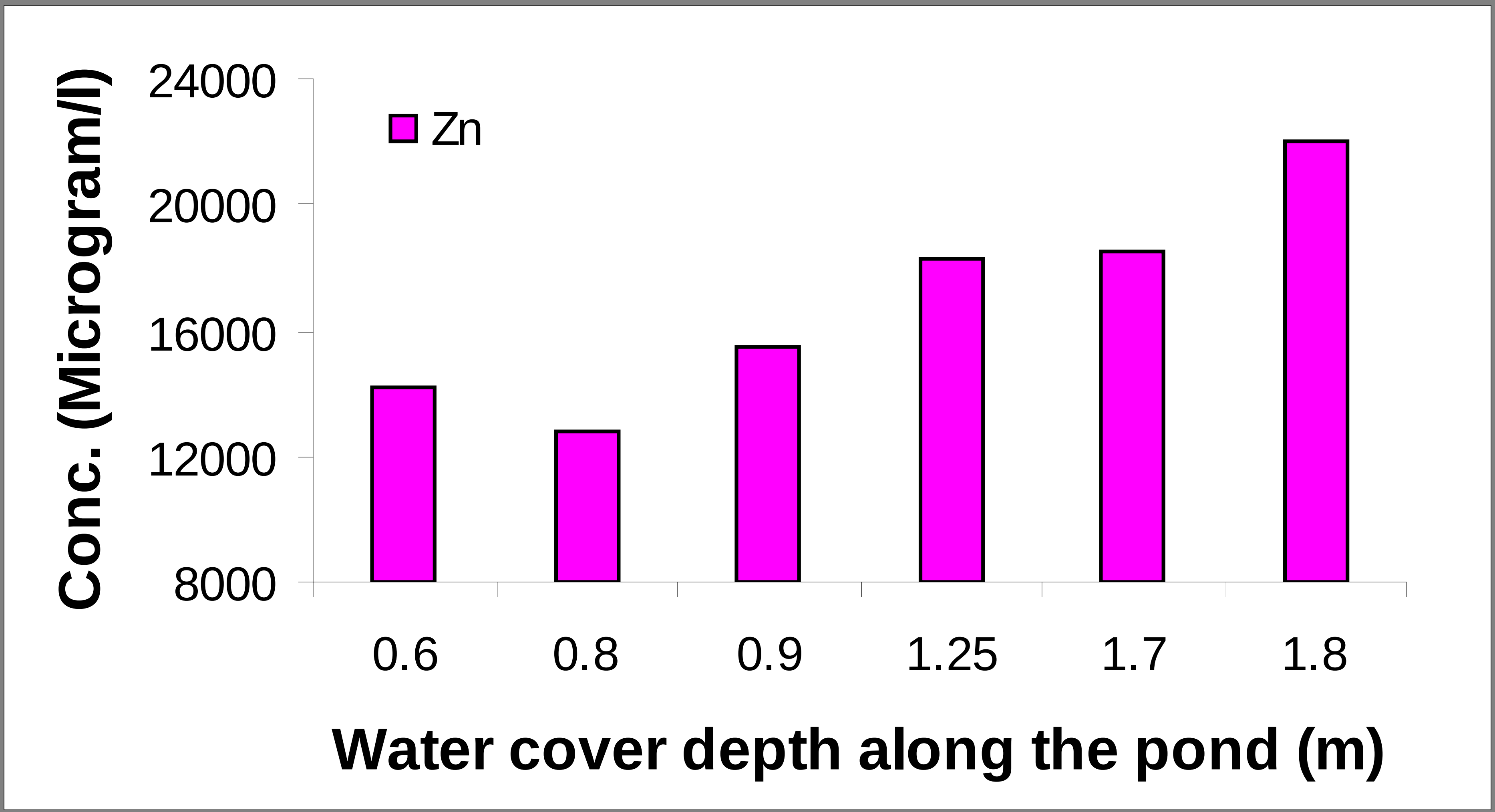

Conc. (Microgram/l)
24000
20000
16000
12000
8000
Zn
0.6
0.8
0.9
1.25
1.7
1.8
Water cover depth along the pond (m)


Cell 14
Evans Lake
Gravel Pit Lake
Effluent Treatment Plant
Settling Ponds
Main Dam
Effluent Discharge
Hwy 108
Serpent River
Quirke I Mine and Mill Site
Former Townsite

Solid Tailings Analysis

Station 1

Top

Oxidized tailings (medium sand)

Un-oxidized Tailings (medium sand)

Bottom

Station 3

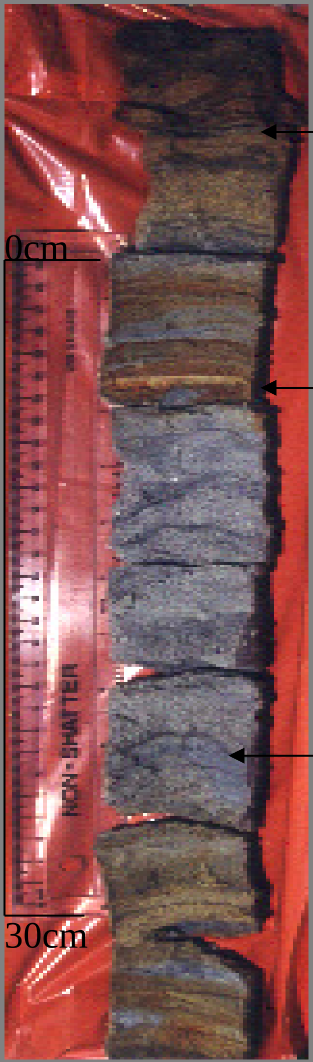

Top

Oxidized tailings (medium sand)

Intermixed fine sand and silt

Un-oxidized Tailings (medium sand)

Bottom

Station 6

Oxidized tailings with organic matter (fine to medium sand)

Gypsum and calcite (silt)

Intermixed fine sand and silt

Bottom

Mineralogical Analysis

Station Number	Main Mineral	Sulphide Mineral	Secondary Mineral	Trace or Minor
1	Quartz (88 to 95%) K-Feldspar (1 to 8%) Muscovite (1 to 3%)	Pyrite (2 to 8%)	Gypsum (2 to 17%) Calcite (1 to 17%)	Chalcopyrite Rutile Illmenite
3	Quartz (65 to 98%) K-Feldspar (3 to 10%) Muscovite (1 to 4%)	Pyrite (1 to 2%)	Gypsum (1 to 4%)	Chalcopyrite Rutile
6	Quartz (69 to 91%) K-Feldspar (3 to 11%) Muscovite (1 to 8%)	Pyrite (2 to 8%)	Gypsum (4 to 18%)	Chalcopyrite Rutile

SO4 Concentration (mg/L)

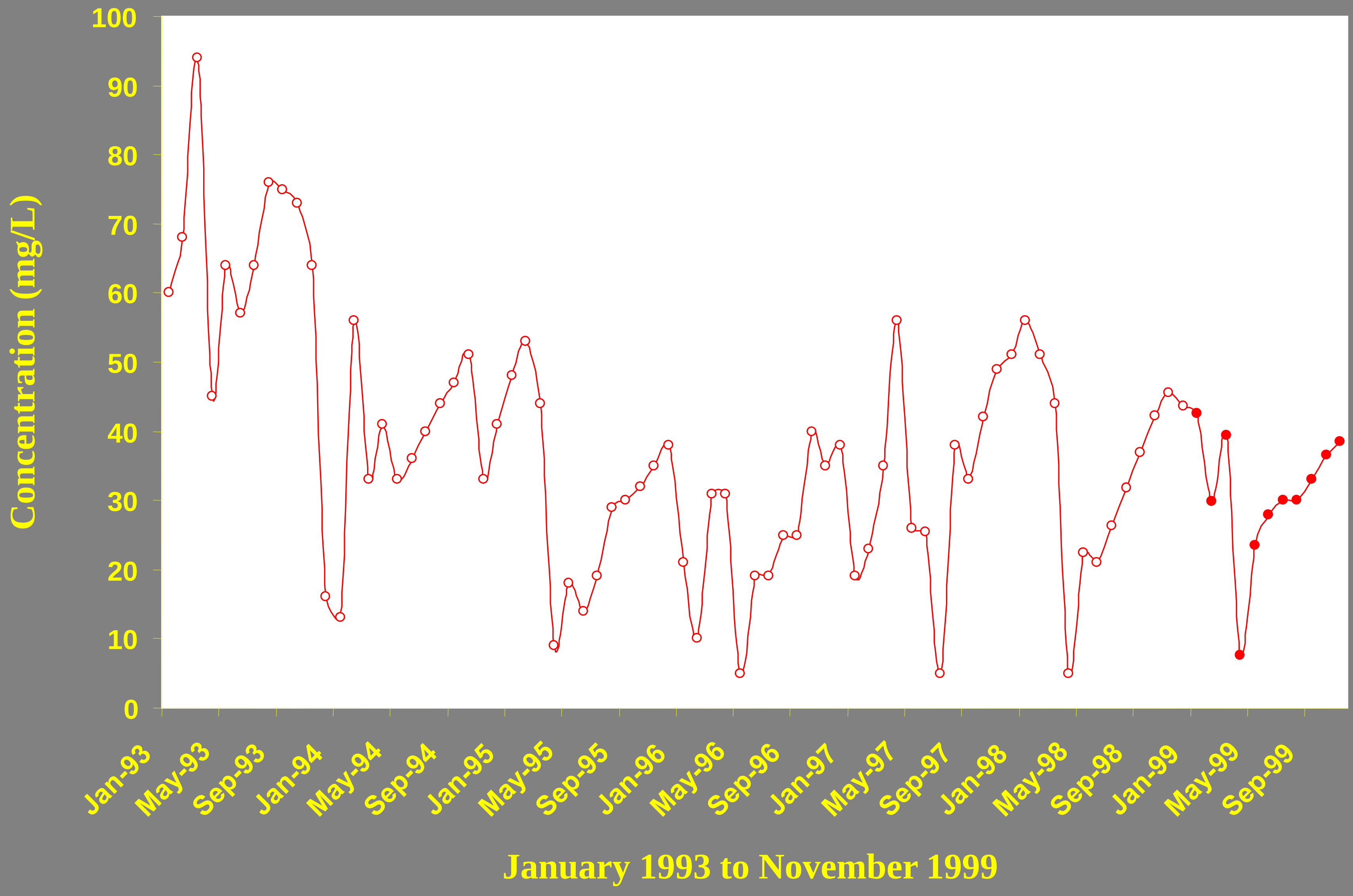

Alkalinity as $CaCO_3$ (mg/L)

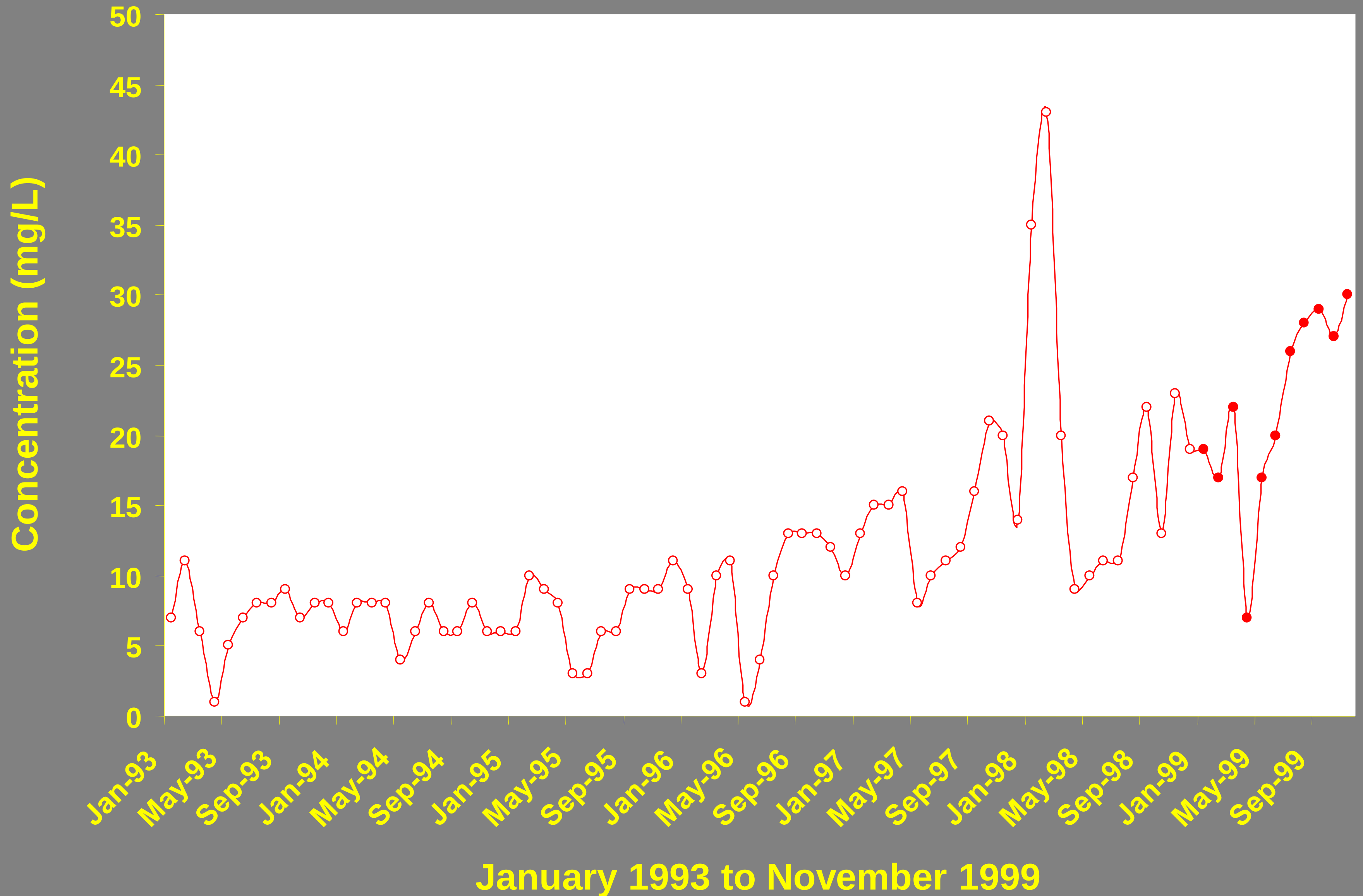

pH

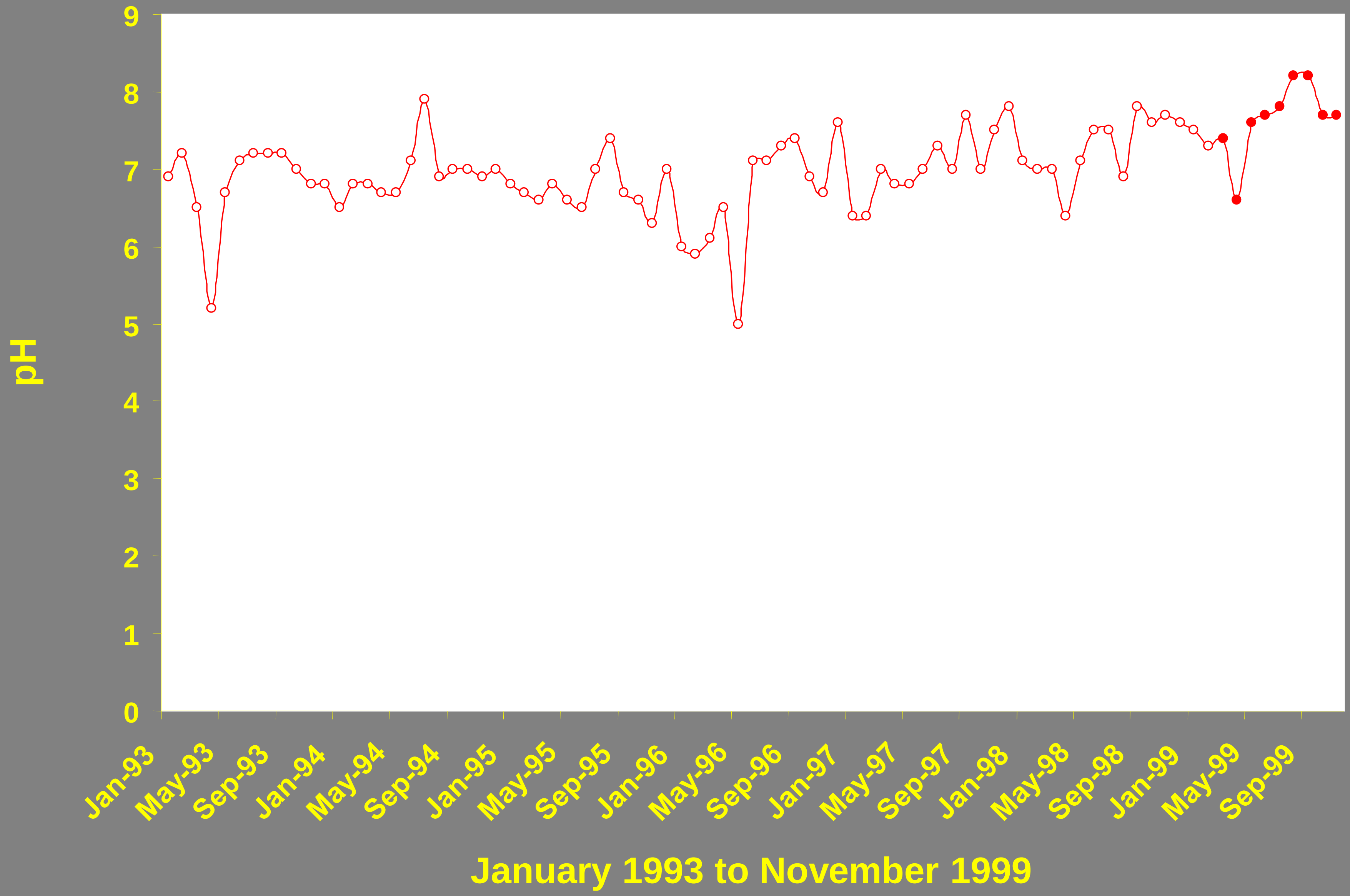

pH
9
8
7
6
5
4
3
2
1
0
Jan-93
May-93
Sep-93
Jan-94
May-94
Sep-94
Jan-95
May-95
Sep-95
Jan-96
May-96
Sep-96
Jan-97
May-97
Sep-97
Jan-98
May-98
Sep-98
Jan-99
May-99
Sep-99
January 1993 to November 1999

Ra-226 Concentration (Bq/L)

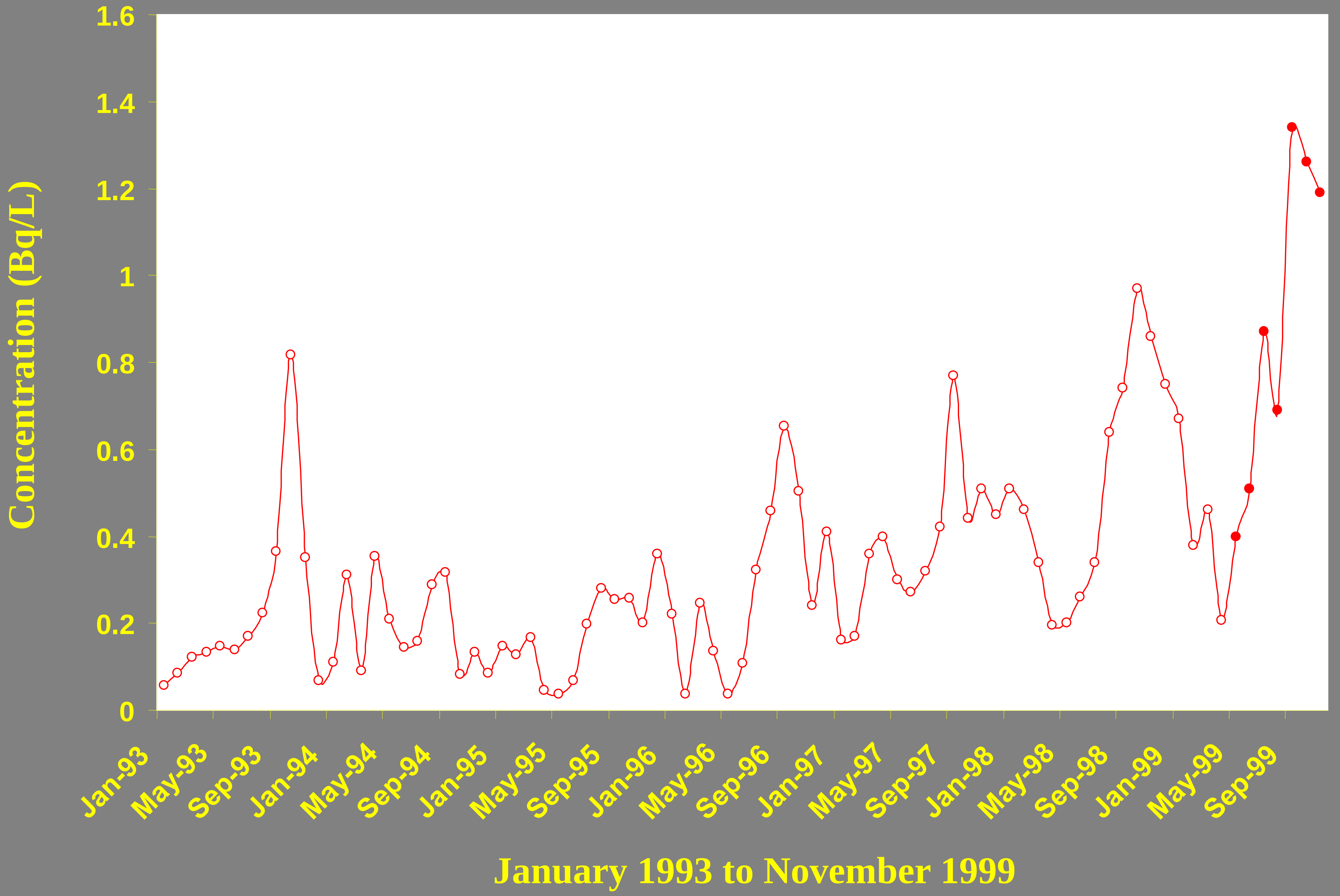

Seepage Loss Analysis

- Golders Associates
- SL=P-E-H
- Fresh water inflow from Gravel Pit Lake to maintain operating elevation of 1310ft
- Factored Precipitation 0.7
- Class A pan evaporation of 0.85
- Dyke 14, two perimeter dams (K1 and K2) and an old landfill
- Seepage for 1993 and 1999 are: 56.1L/sec and 40L/sec

Fluxes in the Water Cover

- Fluxes calculated using the method developed by Catalan, Yanful and St.Arnaud (1999) for Preoxidized Tailings.

- $F_T = F_A + F_N$

- $M_W(t_2) - M_W(t_1) = F_T \Omega.(t_2 - t_1)$

- $F_A = -[1/\ \Omega.(t_2 - t_1)]\ {}_{t1}\int^{t2} SC_W.dt$

- $F_N = 1/\ \Omega.(t_2 - t_1)\left[M_W(t_2) - M_W(t_1) + {}_{t1}\int^{t2} SC_W.dt\right]$

1993 and 1999 Net Flux of SO_4^{2-}

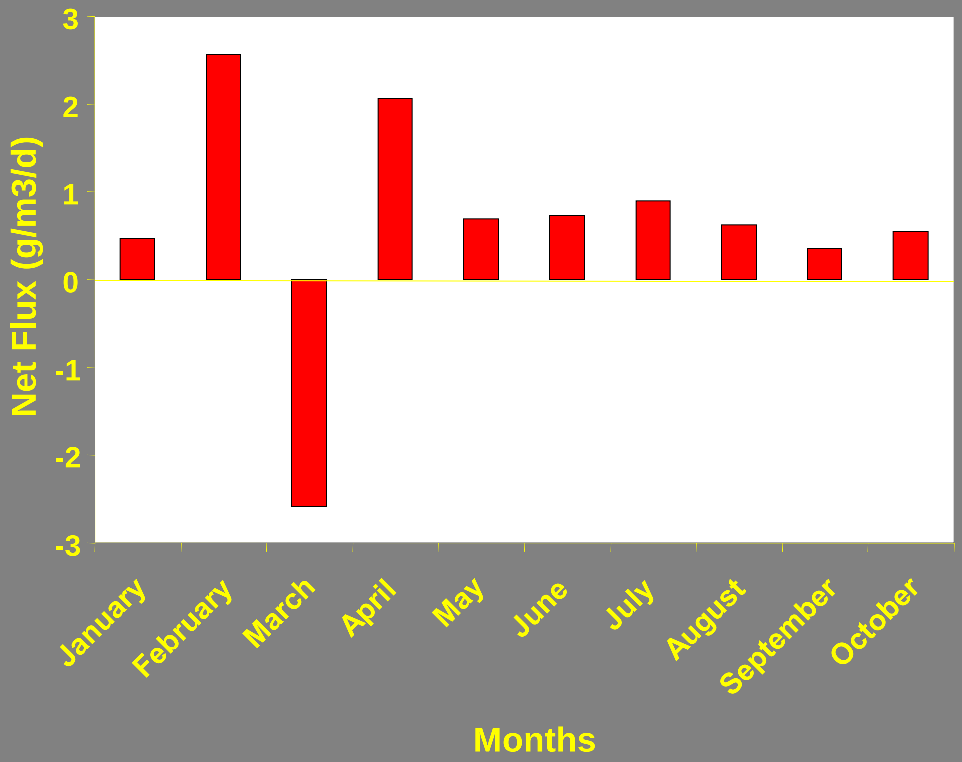

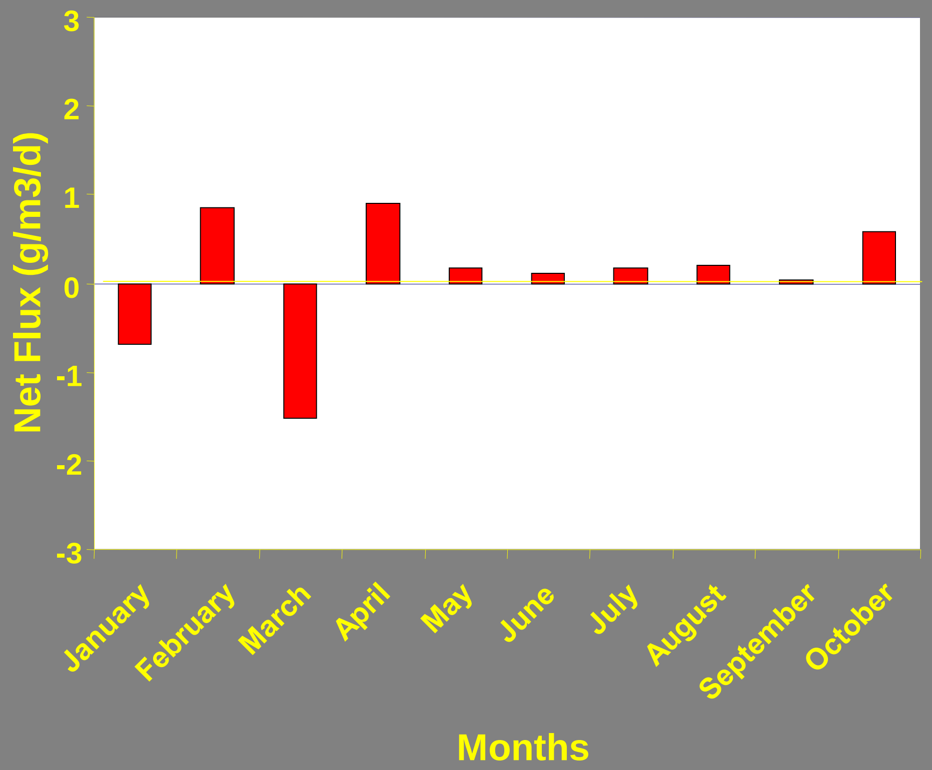

Net Yearly Average Flux of SO_4^{2-}, Ra-226, and TDS

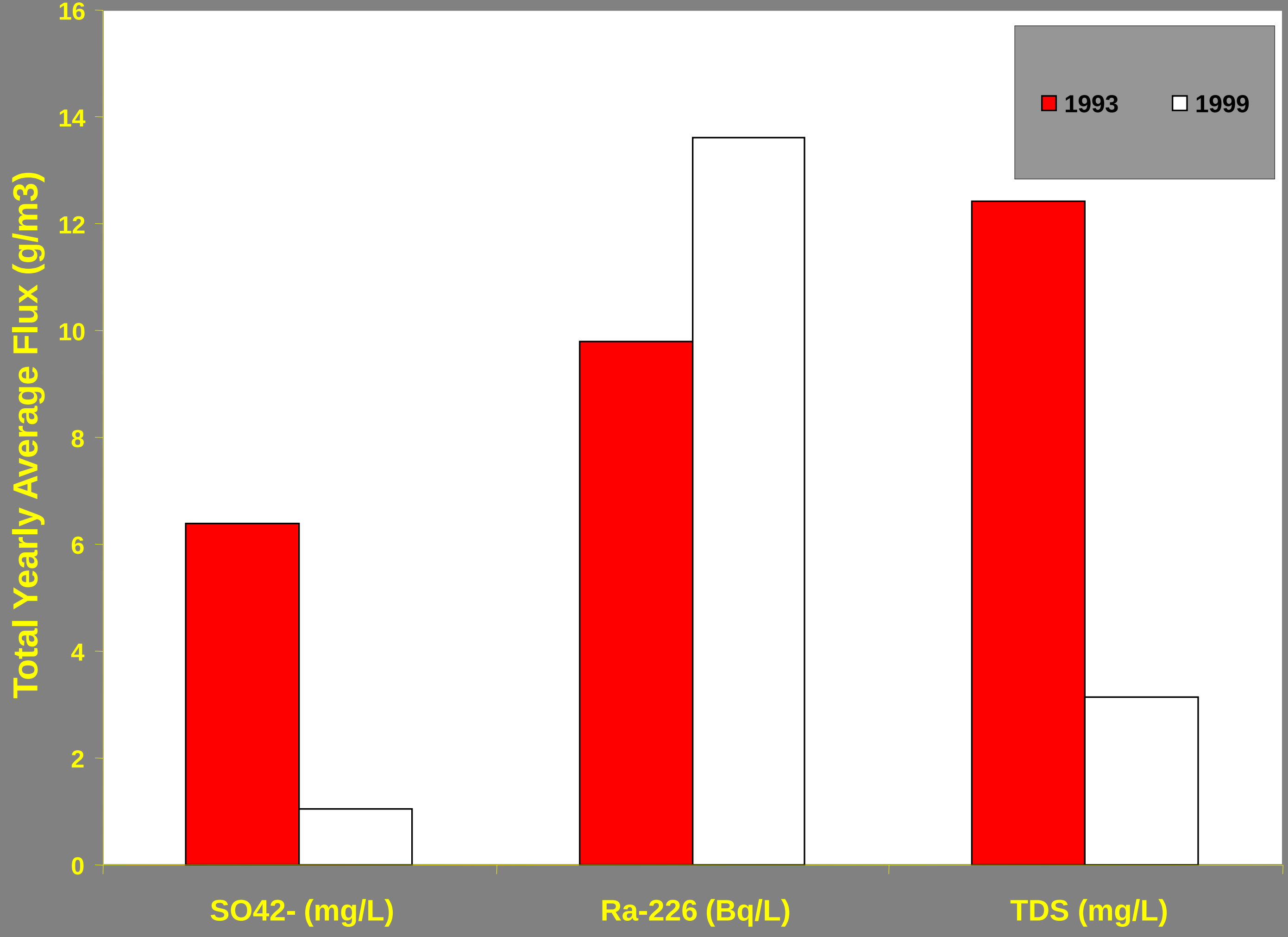

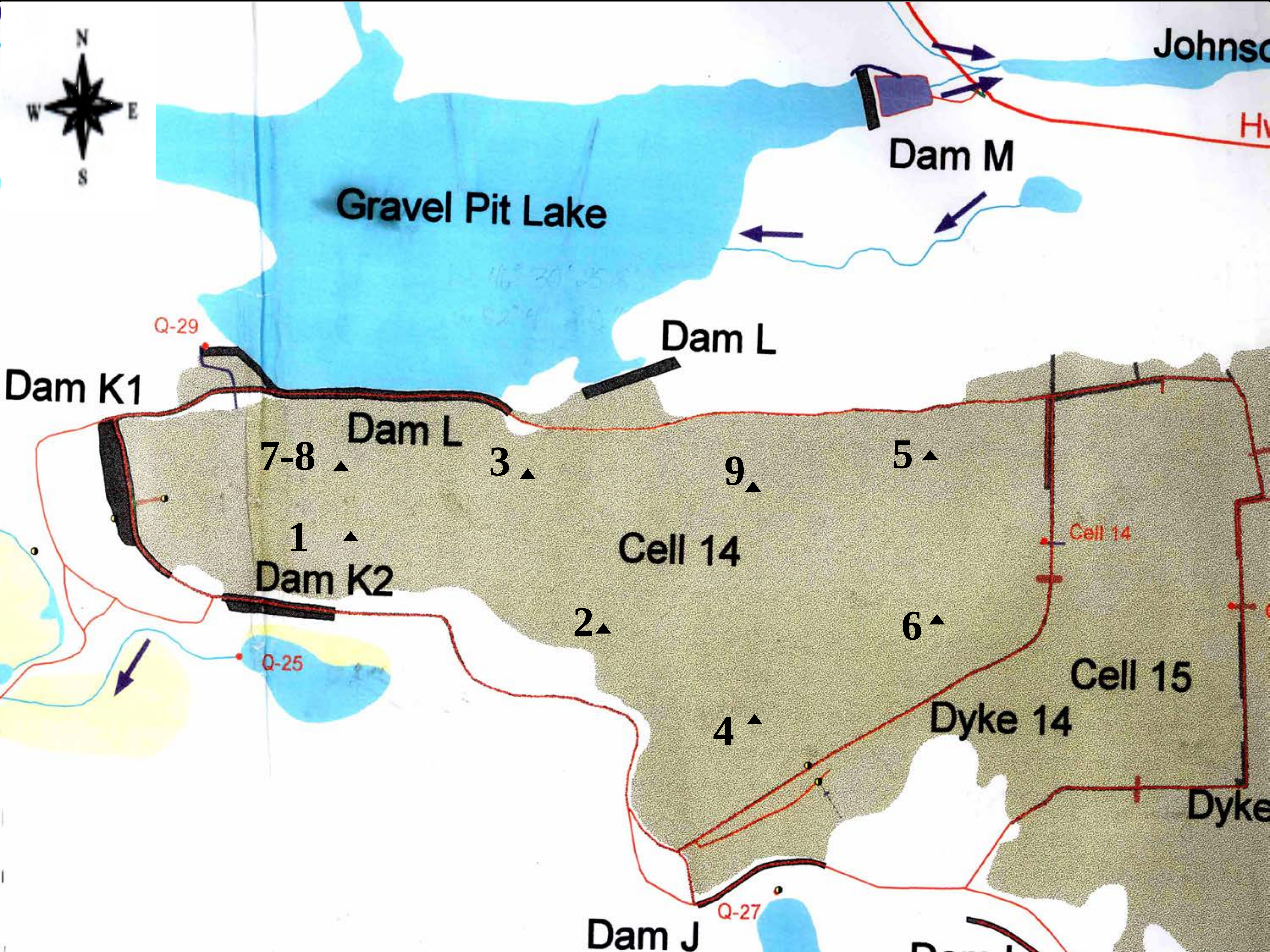
N
W
E
S
Gravel Pit Lake
Dam M
Q-29
Dam K1
Dam L
Dam L
7-8
3
9
5
1
Cell 14
Cell 14
Dam K2
2
6
Q-25
Cell 15
Dyke 14
4
Q-27
Dam J

Predicted bed shear stress

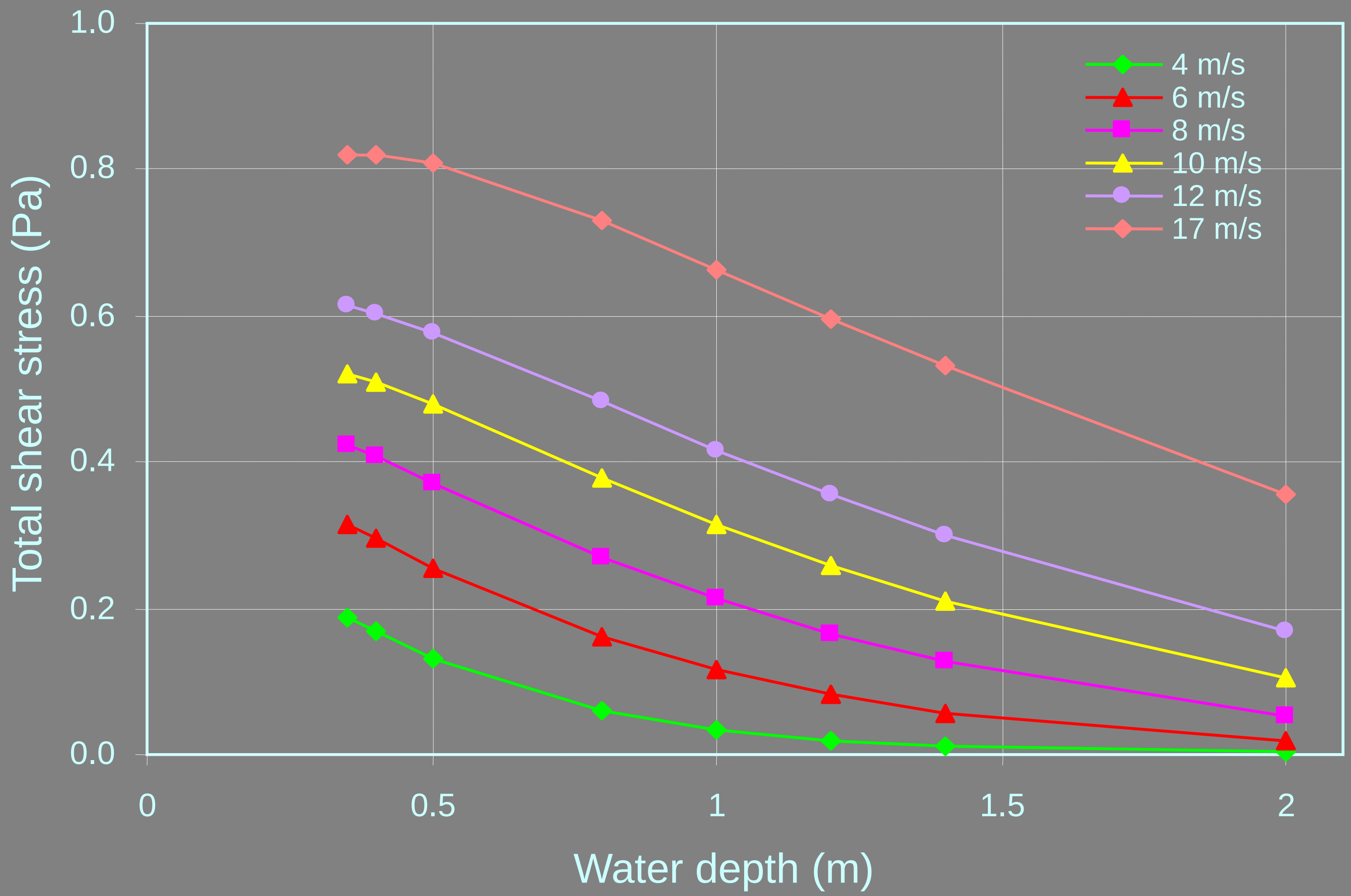

critical shear stress

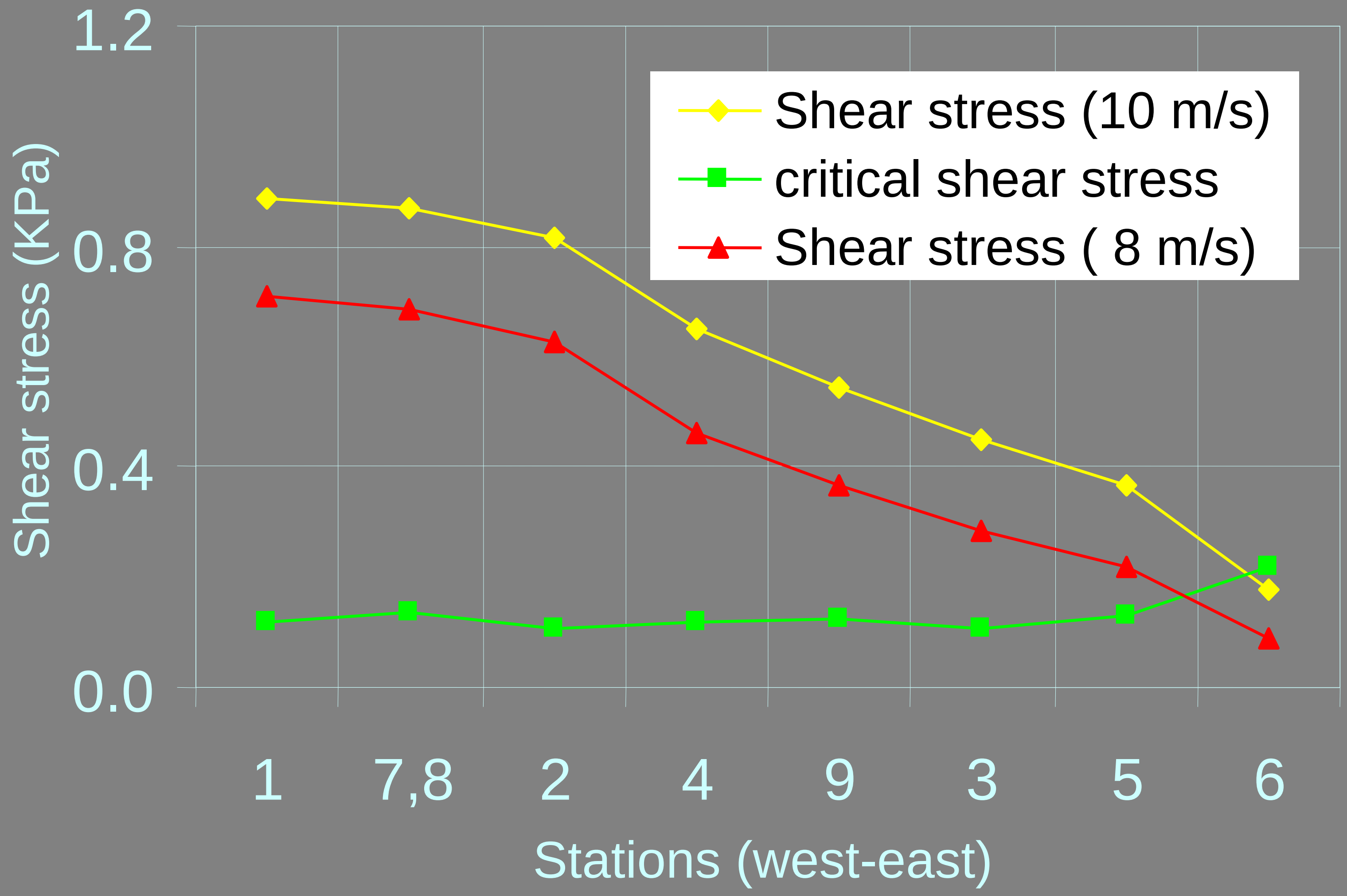

Dry mass of suspended sediments at different depths

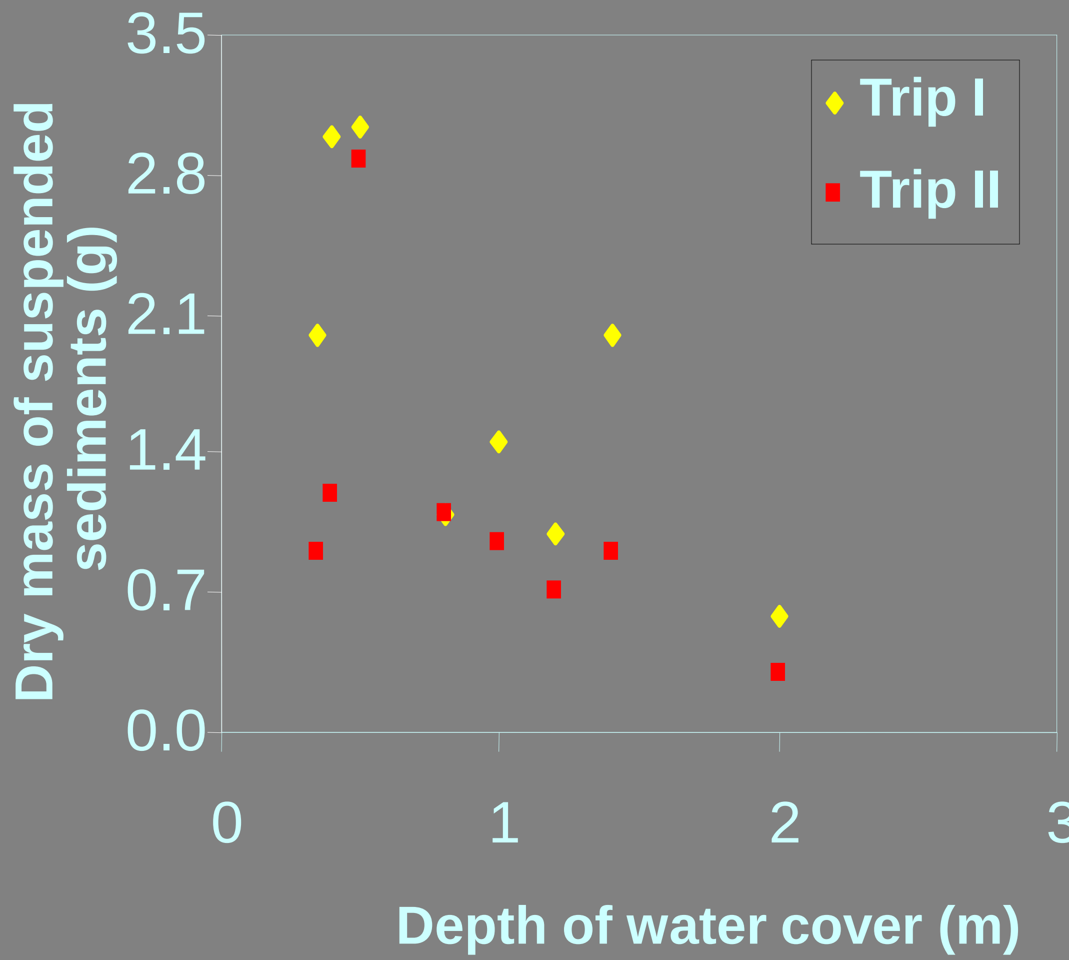

- mass of suspended solids decrease with increasing water depth.

Comparison of D_{50} of bed and suspended tailings

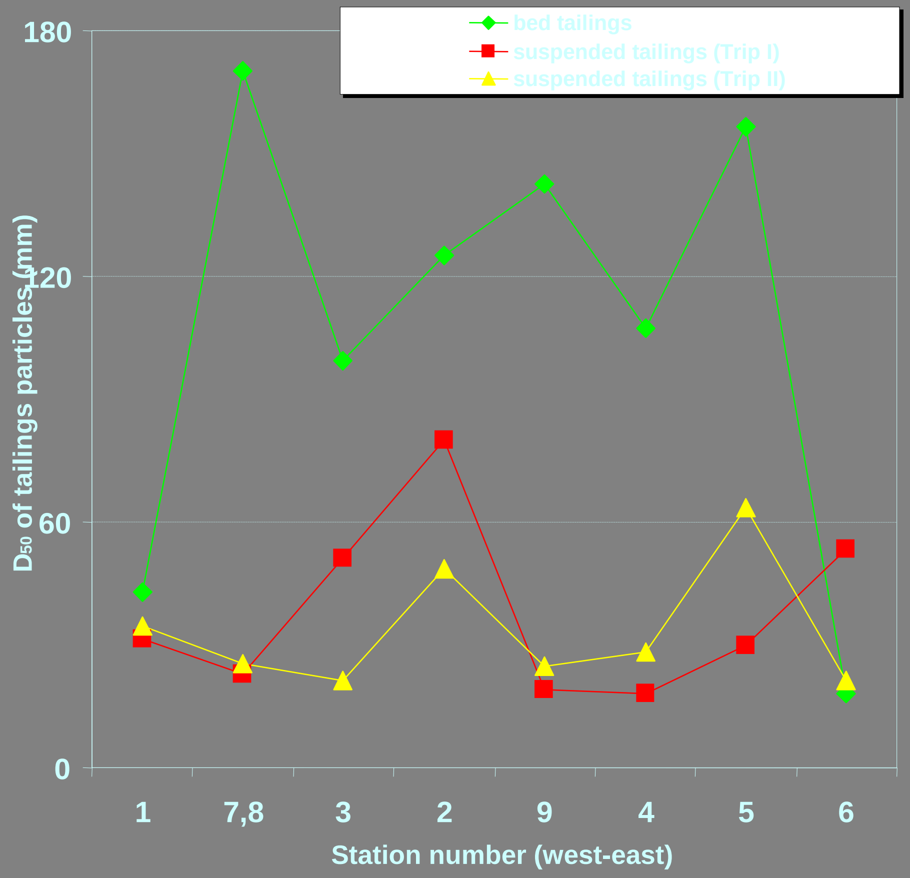

- Particle sizes of the suspended tailings were much finer than that of the bed tailings.

- Suspended tailings for Trip II were coarser than for Trip I, (stronger wind conditions, creating higher bottom stresses).

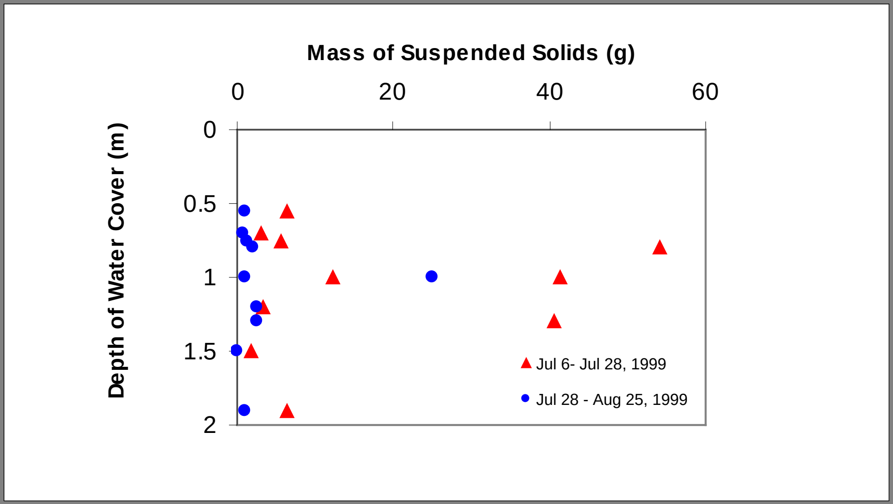

Heath Steele
Upper Cell

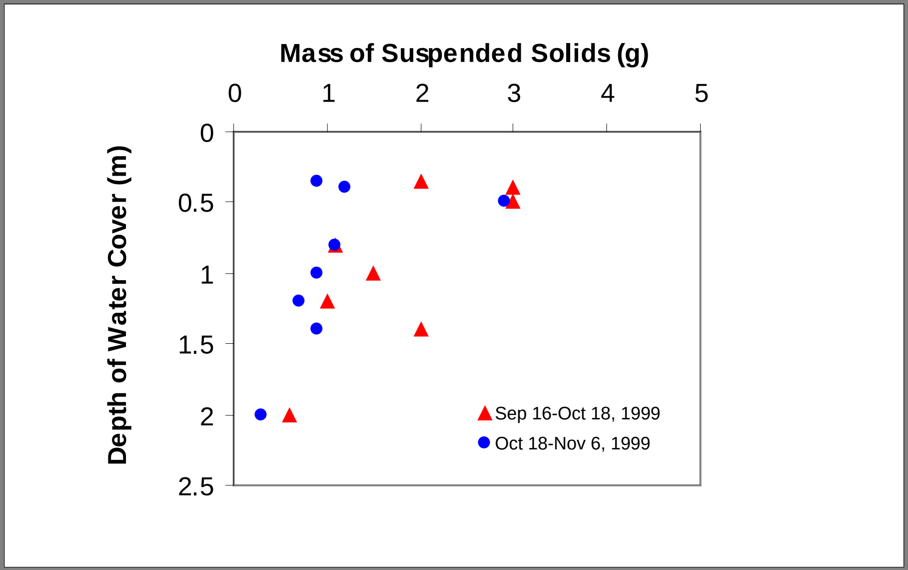

Quirke Cell #14

Mineralogical composition of bed and suspended tailings

Minerals	Chemical composition	Percentage estimation	
		Bed tailings	Suspended tailings
Quartz	SiO_2	90	93
Mica	$KAl_2AlSi_3O_{10}(OH)_2$	2.5	1.3
Calcite	$CaCO_3$	3.5	0.25
Pyrite	FeS_2	1.5	1
Feldspar	$KAlSi_3O_8$	3.5	3.9

Elemental composition of bed and suspended tailings

Bed tailings																		
Station	Si	Ti	Al	Fe	Mn	Mg	Ca	K	P	Na	Cd	Cu	Ni	Pb	Zn	S	Th	U
1	397979	2618	22985	23641	129	3417	1644	18402	626	0	1	57	19	191	21	16563	97	18

Suspended sediments (Trip I)																		
Station	Si	Ti	Al	Fe	Mn	Mg	Ca	K	P	Na	Cd	Cu	Ni	Pb	Zn	S	Th	U
1	310959	2338	29712	78337	1239	2593	1715	19675	393	0	3	234	42	946	484	25880	264	55

Suspended sediments (Trip II)																		
Station	Si	Ti	Al	Fe	Mn	Mg	Ca	K	P	Na	Cd	Cu	Ni	Pb	Zn	S	Th	U
1	334598	2878	28335	53087	1007	2231	18511	19342	175	0	1	120	45	673	104	10910	262	42

New Tailings Area (Upper Terrace)

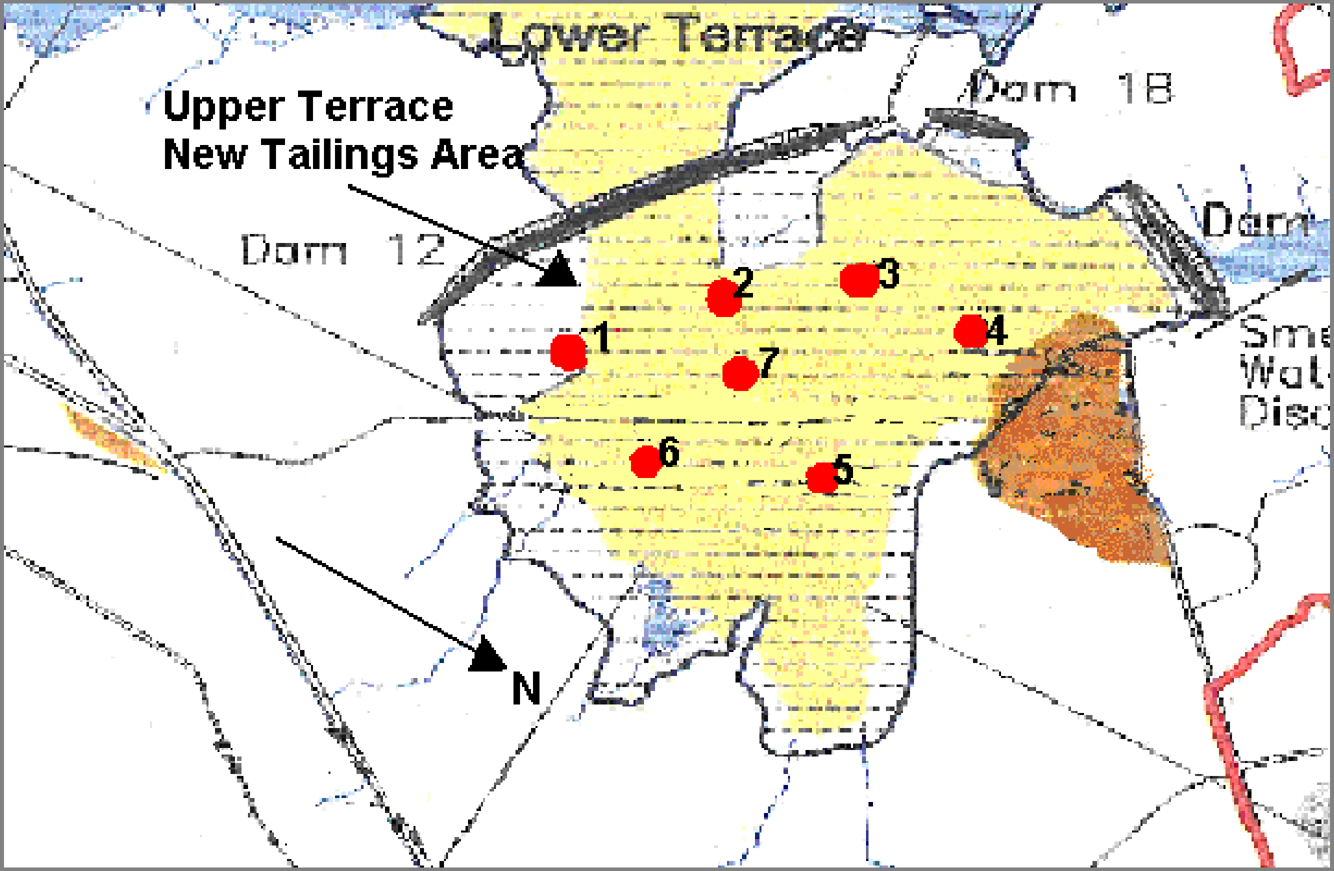

Depth of Water Cover vs Average Grain Size

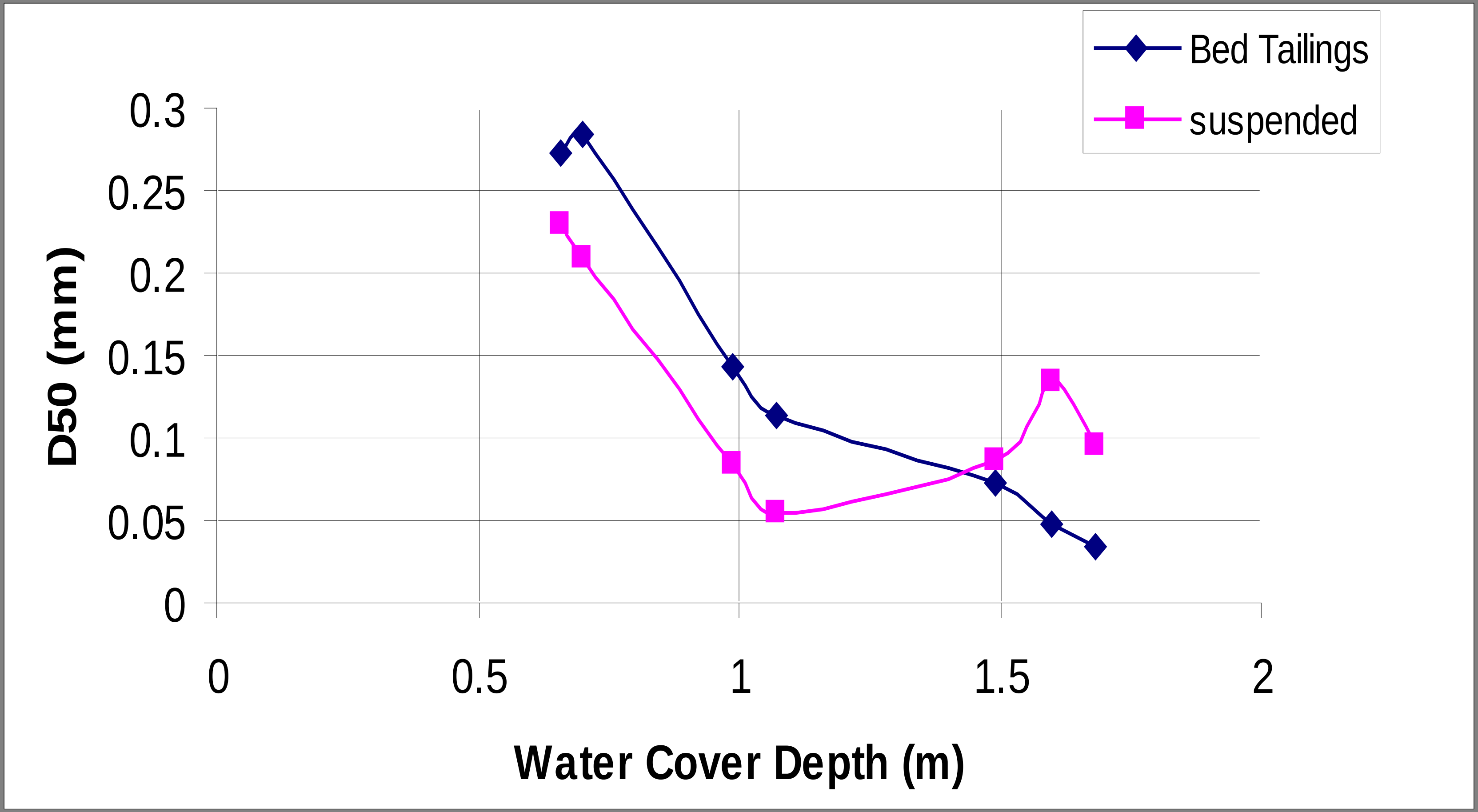

Total Mass of Collected Material with Depth of Water Cover

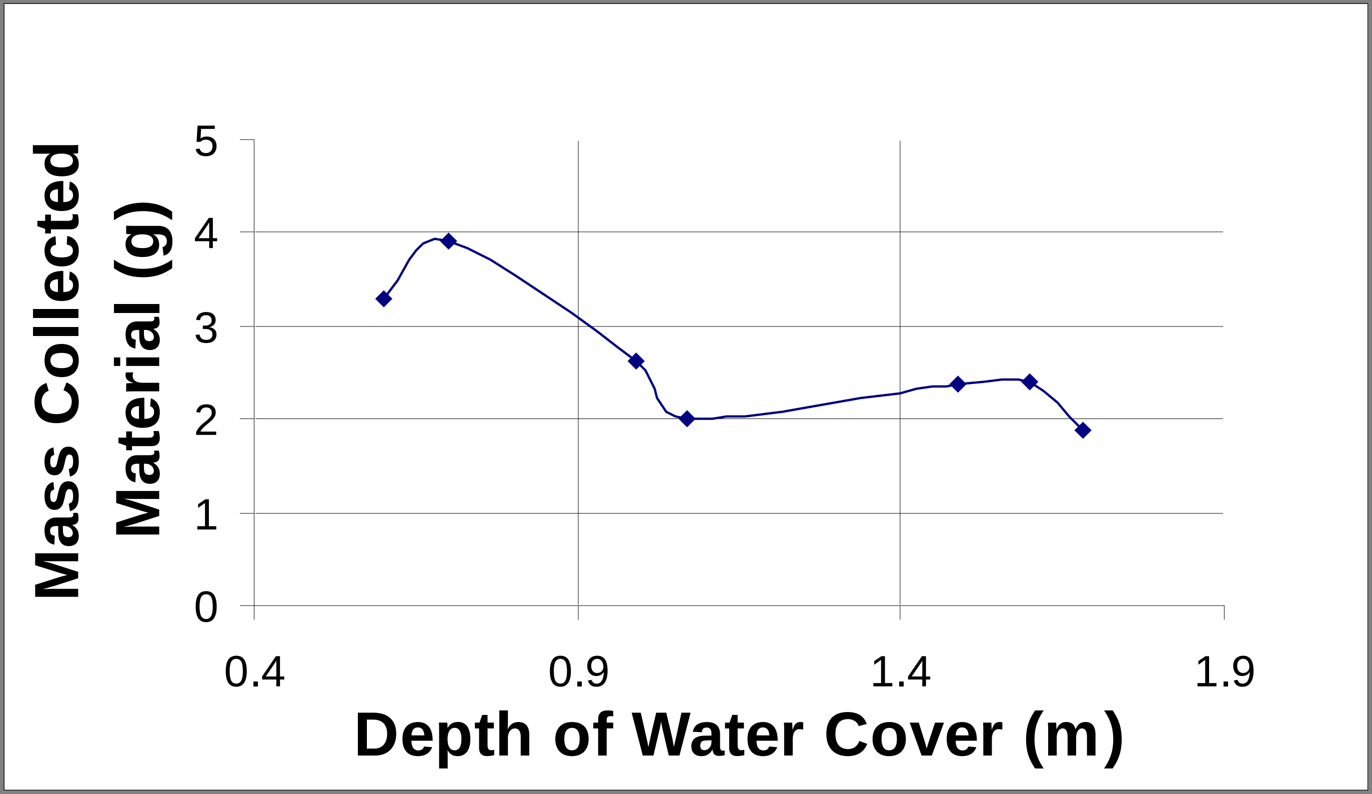

Elemental Analysis

	Nitrogen (%)	Organic Carbon (%)	Sulfur (%)
Average Bed Tailings	0.01	0.17	3.16
Averaged Collected Tailings	0.8	7.47	1.39

Wave Tank Assembly

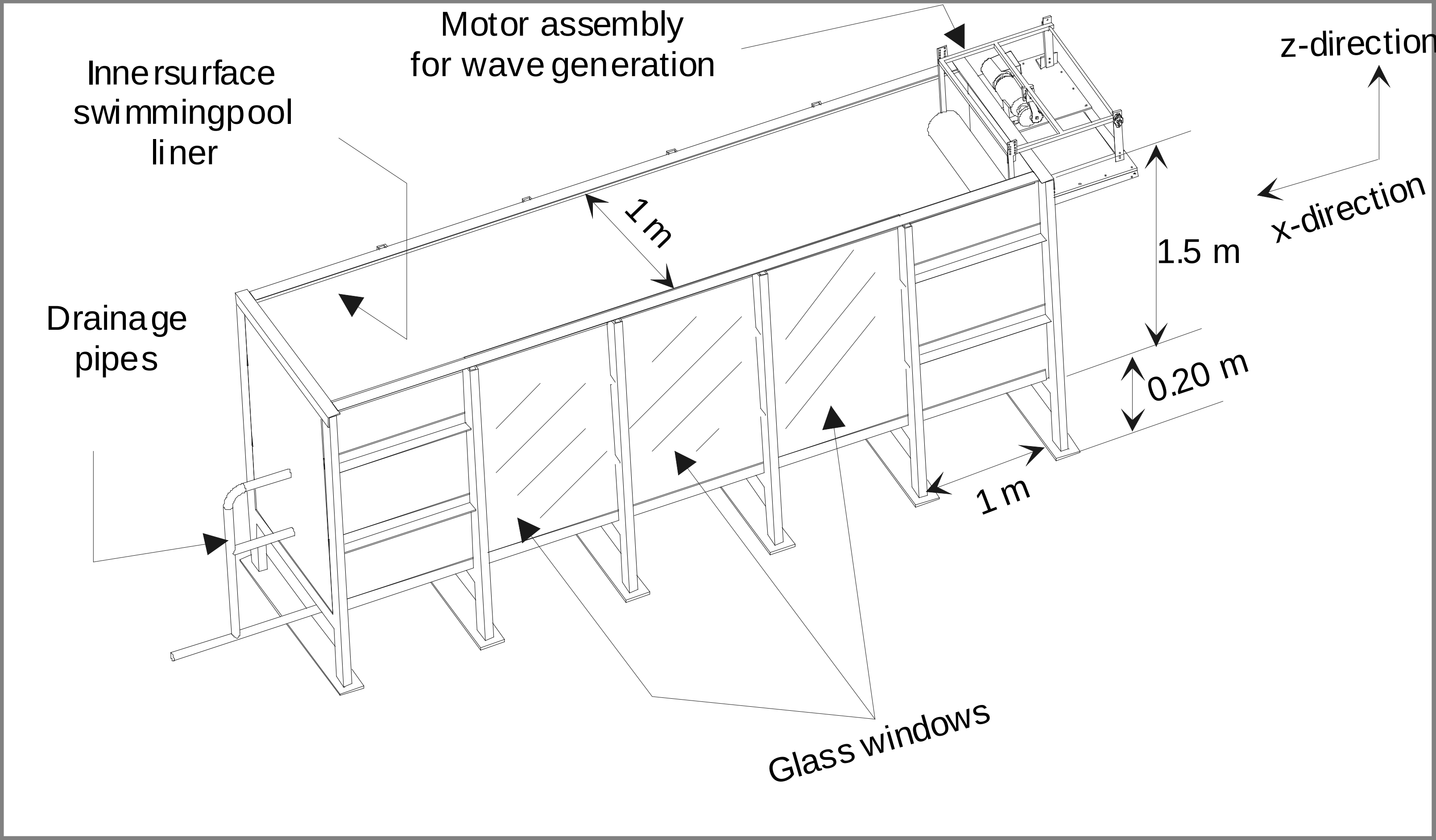

Photograph

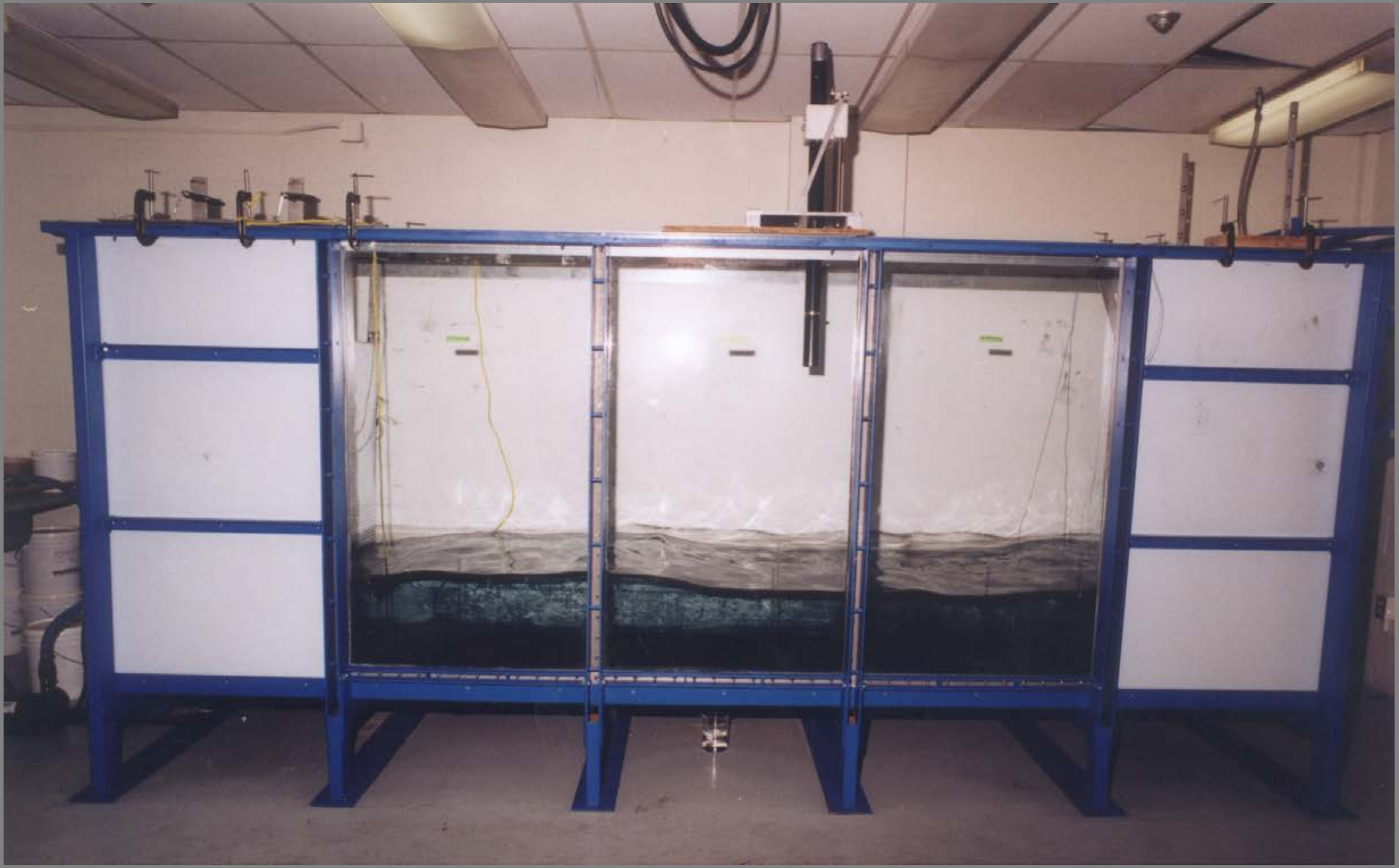

Tank settings for resuspension experiments

Parameters	Values
Cylinder diameter	0.20 m
Wave height (H)	0.07 m
Wave frequency	0.622 Hz
Water level (h)	0.35 m
H/h ratio	**0.20**
Wave length (L)	2.70 m
Celerity (C)	1.76 m/s

Oxidation rate from shake flask

$$FeS_2 + 3.75\ O_2 + 3.5\ H_2O \rightarrow Fe(OH)_3 + 2\ SO_4^{2-} + 4\ H^+$$

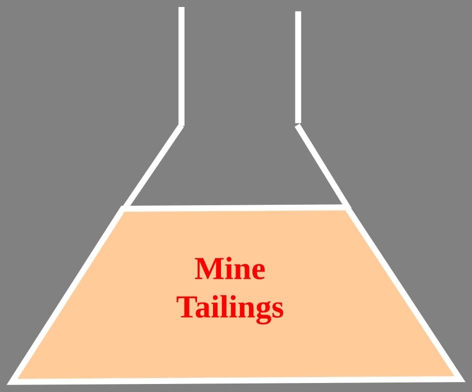

Shake flask

$$\frac{dC_{SO_4^{2-}}}{dt} = -\frac{2}{3.75}\frac{dC_{O_2}}{dt}$$

47 mg SO_4^{2-} L^{-1} day^{-1}

220 x 10^{-9} mole SO_4^{2-} $kg^{-1}s^{-1}$

60.73 x 10^{-10} mole O_2 m^{-2} s^{-1}

Diffusion model

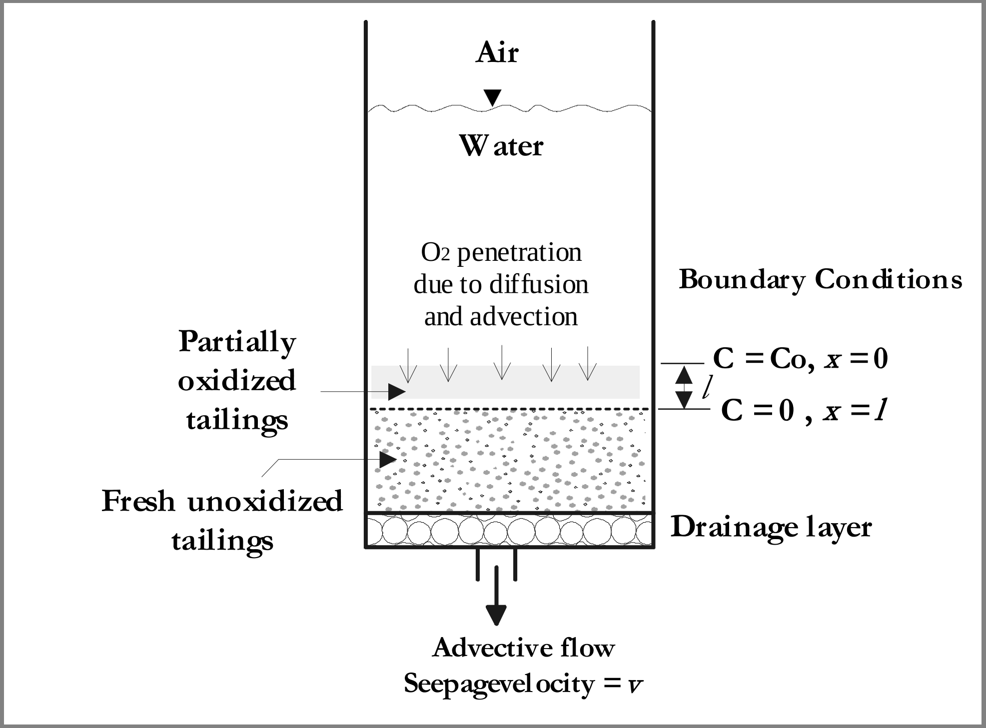

- Completely mixed water
- No resuspension
- Advection

$$\frac{\partial C}{\partial t} = D_1^* \frac{\partial^2 C}{\partial x^2} - v\frac{\partial C}{\partial x} - K_1^* C$$

$$flux = -\frac{v}{2} C_0 \left(1 - \sqrt{1 + \frac{4K_1^* D_1^*}{v^2}} \right)$$

Model representing experimental tanks

Sulphate production rate from the wave tank	=	Background sulphate concentration	+	Sulphate produced due to resuspension of tailings	+	Sulphate produced due to diffusion of oxygen into submerged tailings

$$\left(\frac{mgSO_4^{-2}}{L}\right) = C_b + \frac{10 \times s \times a_0}{h \times t_d^{\alpha}} T_t \left(\frac{\tau - \tau_c}{\tau_c}\right)^{\beta} + \frac{1.3824 \times 10^8 \times T_t \times C_0 \sqrt{D^* K^*}}{h}$$

Sulphate concentration

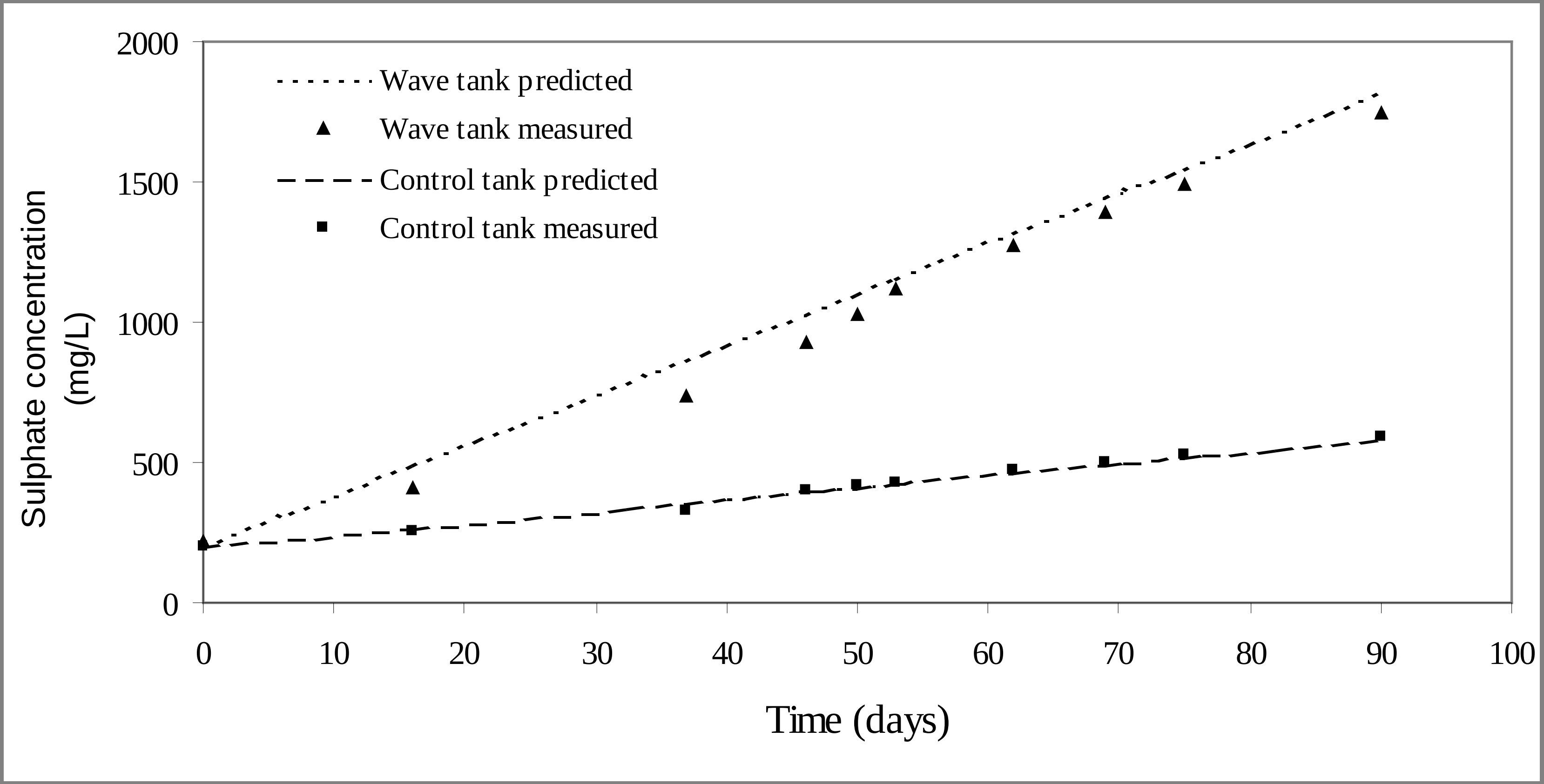

Study of surface **shear** and **waves** induced countercurrent flow

- Experimental Study
- Mathematical modeling

Classification of waves

- **Deep: h/λ>1/2**
- **Intermediate: 1/20<h/λ<1/2**
- **Shallow: h/λ<1/20**

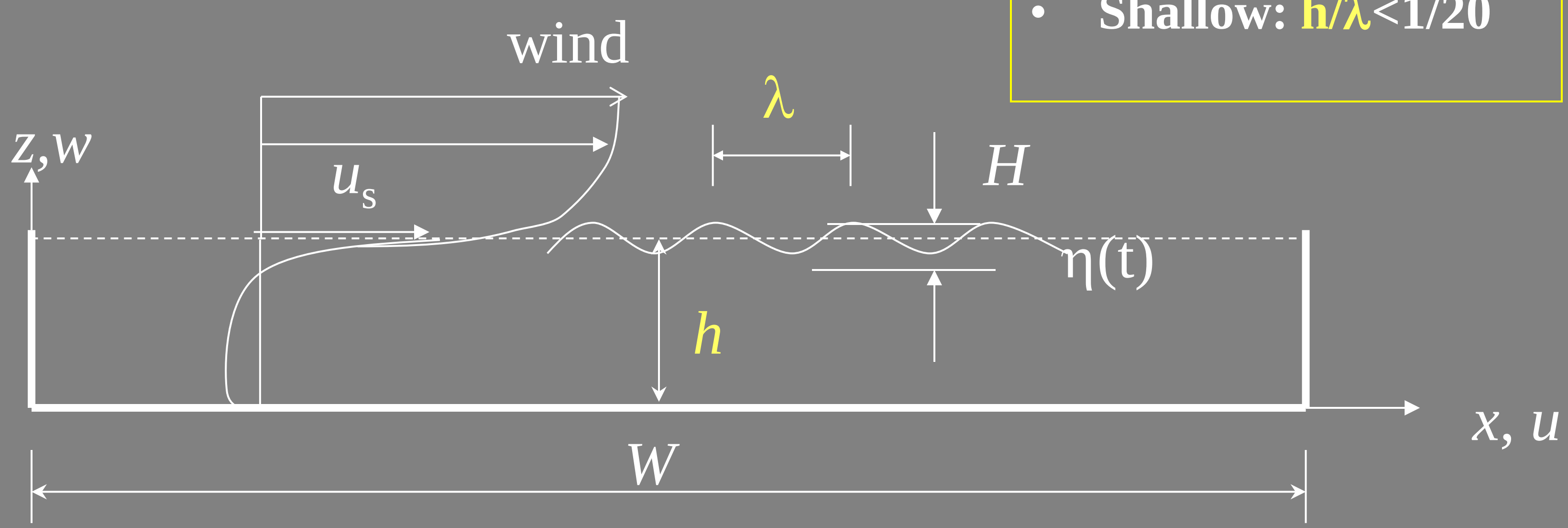

Experimental study

Controlled wind speed, water depth,

Closed-circuit wind-wave tunnel in Boundary Layer Wind Tunnel Laboratory, the University of Western Ontario, London, Ontario, Canada

Schematic of wind-wave tunnel

Measurements:

- Wind speed
- Wave height
- Pressure
- Velocity of water

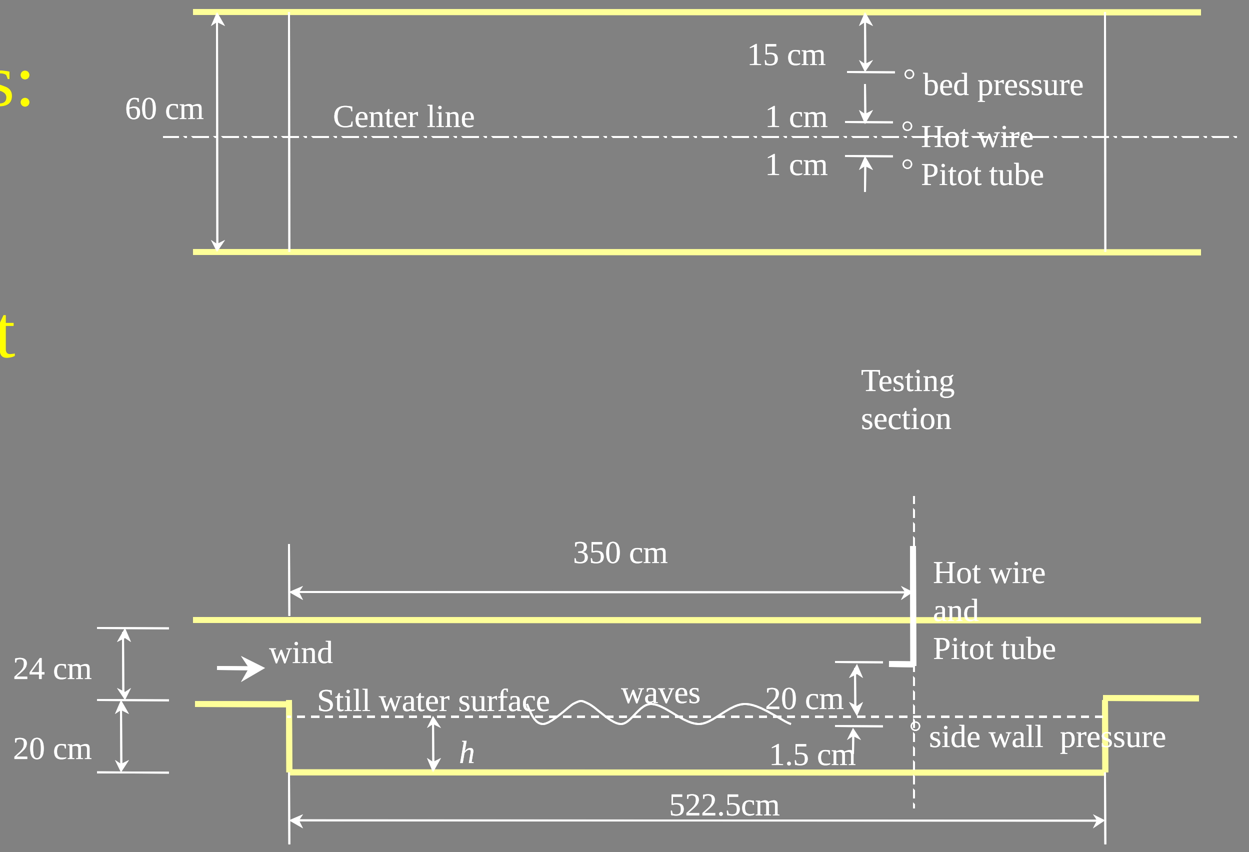

Objective

- Describe the impact of surface wind-waves on the flow structure;
- Develop a simple mathematical model to describe the flow motions.

Classification of measured waves

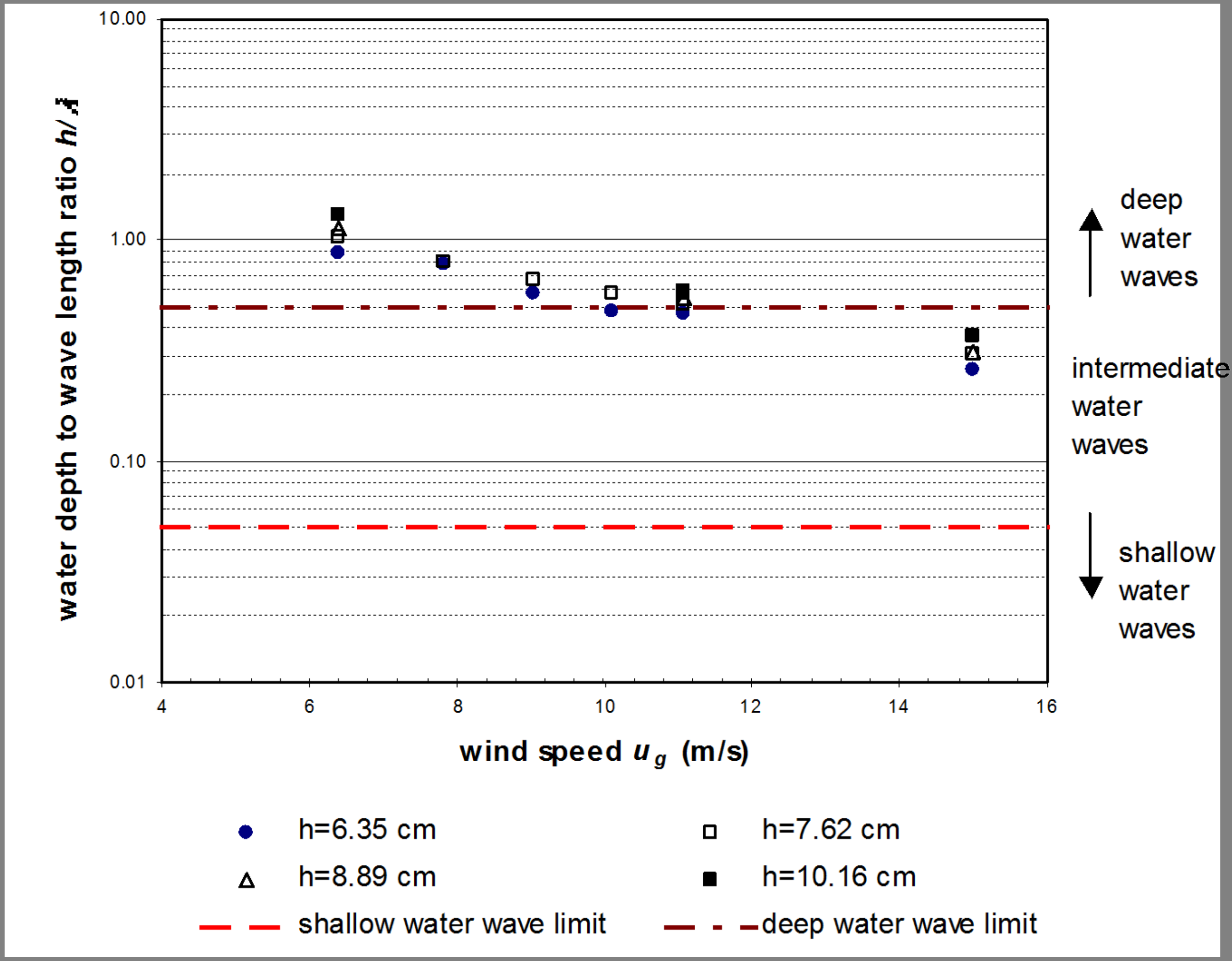

Water surface and bottom pressure correlation versus wind speed

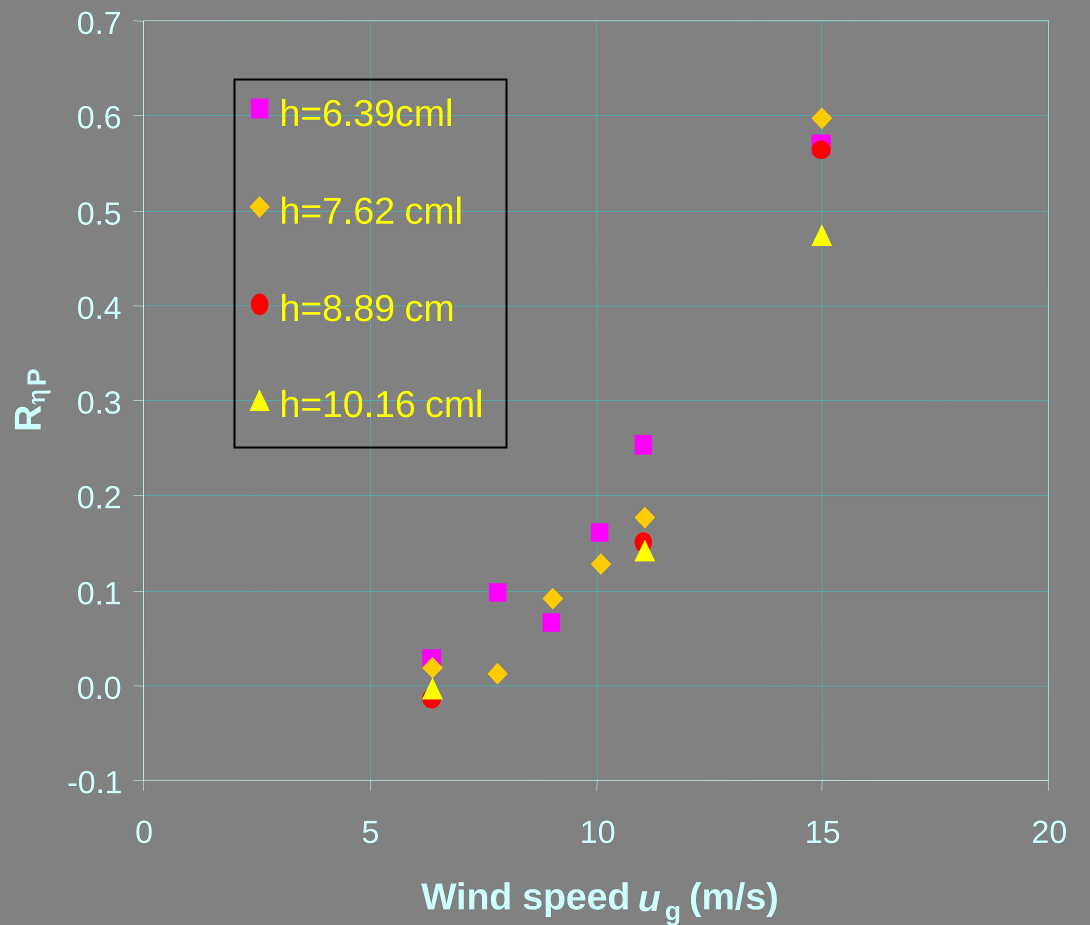

Comparison btwn measured and existed model predicted mean velocity $\overline{u}$ in vertical plane

Deep water-wave

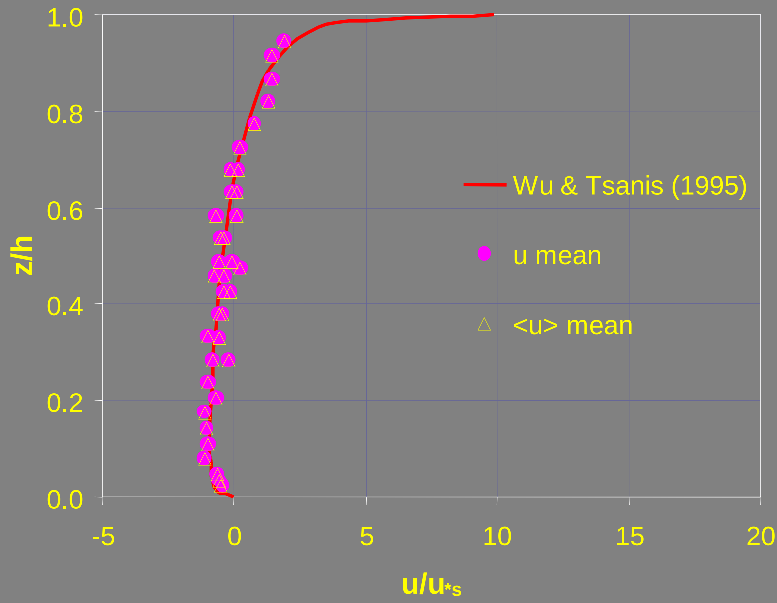

Intermediate water-wave

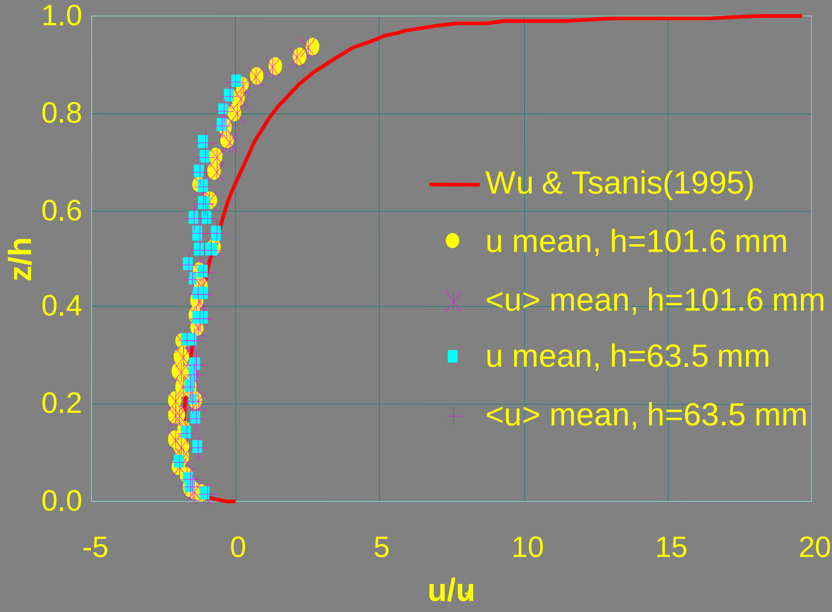

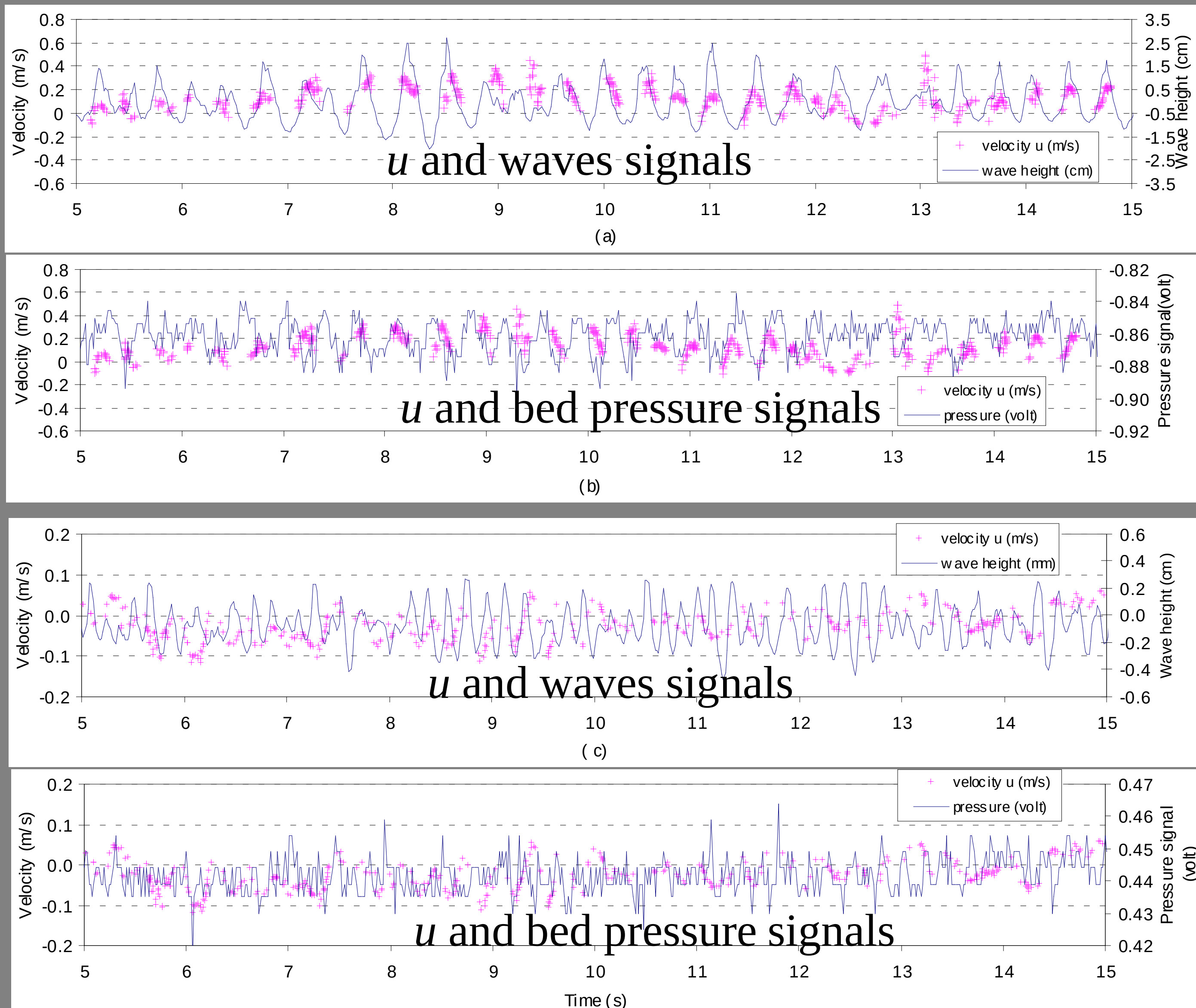

Intermediate water waves: Periodic flow motion

Deep water waves: Non-periodic Flow motion

Triple Decomposition Theory

Hussain and Reynolds (1970)

$$f(x,t) = \bar{f}(x) + f_c(x,t) + f_r'(x,t) = < f(x,t) > + f_r'(x,t)$$

$$\bar{f}(x) = \lim_{T_0 \to \infty} \frac{1}{T_0} \sum_{n=0}^{n=N} f(x,t)dt$$

$$< f(x,t) > = \lim_{N \to \infty} \frac{1}{N} \sum_{n=0}^{n=N} f(x, t + nT)$$

$$f_c = < f > - \bar{f}$$

Wave, velocity signals and selected triggers for a typical experimental record

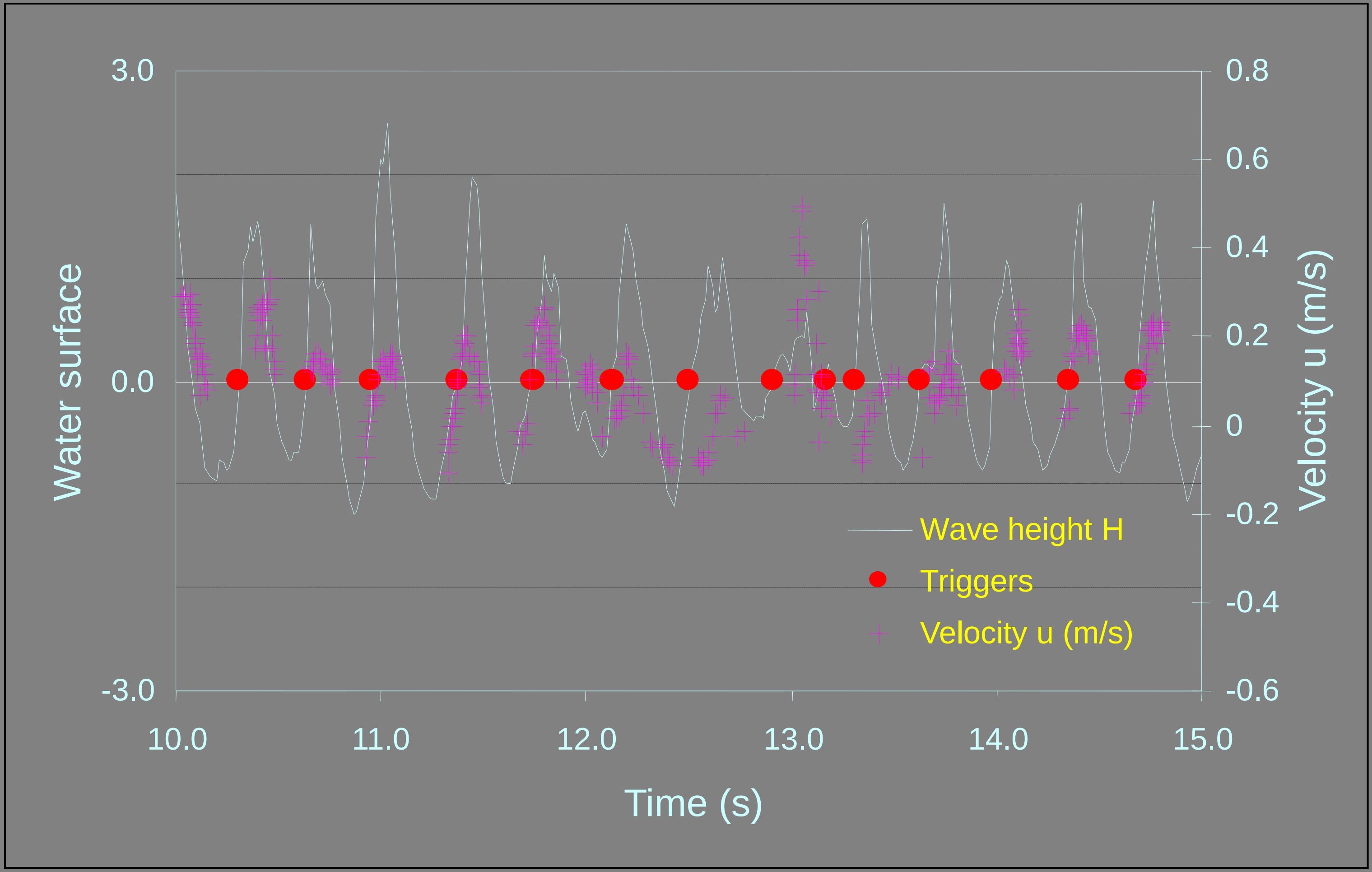

Phase averaged velocity
in vertical plane
during acceleration (t/T=0.325) and
deceleration (t/T=0.875):

(a) Deep water waves
h=63.5 mm

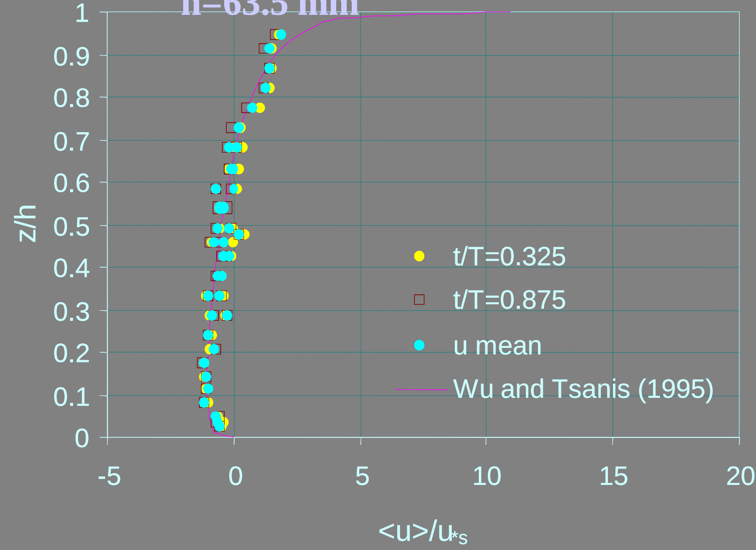

(b) Intermediate water waves
h=63.5 mm

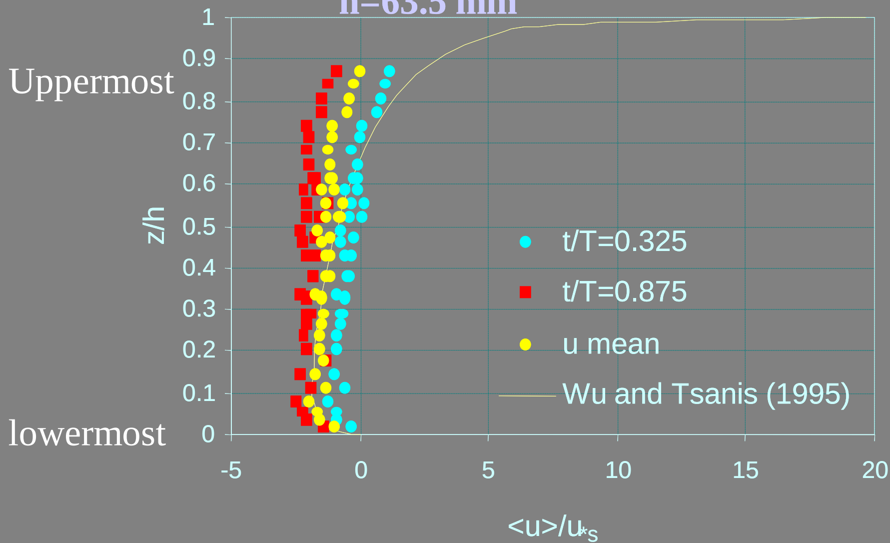

(c) Intermediate water waves
h=101.6 mm

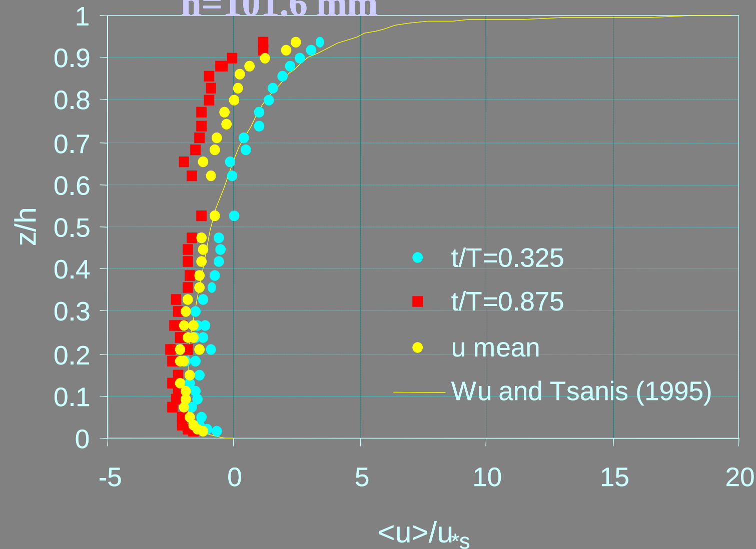

intermediate
water-wave

deep
water-wave

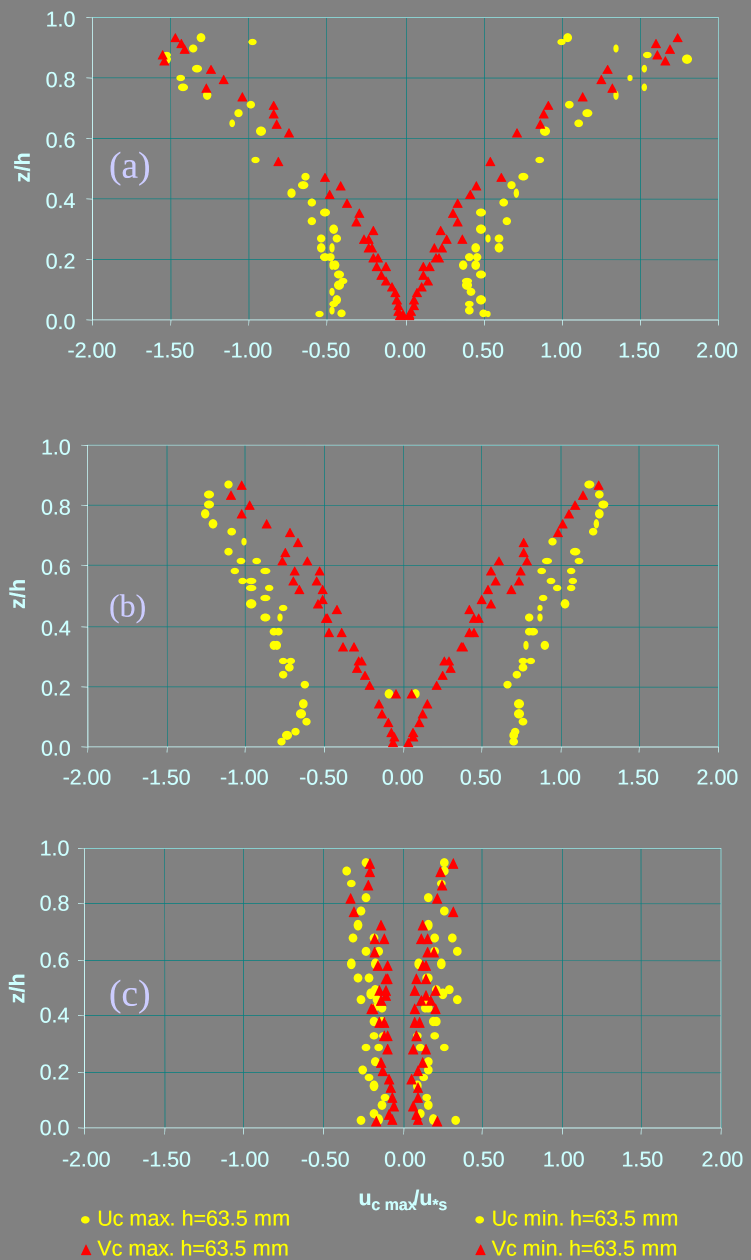

Max. & min. *coherent* velocity components in vertical plane.

Intermediate: Significant

Deep: negligible

Phase-averaged velocity <*u*> varies in a wave period (intermediate water wave conditions)

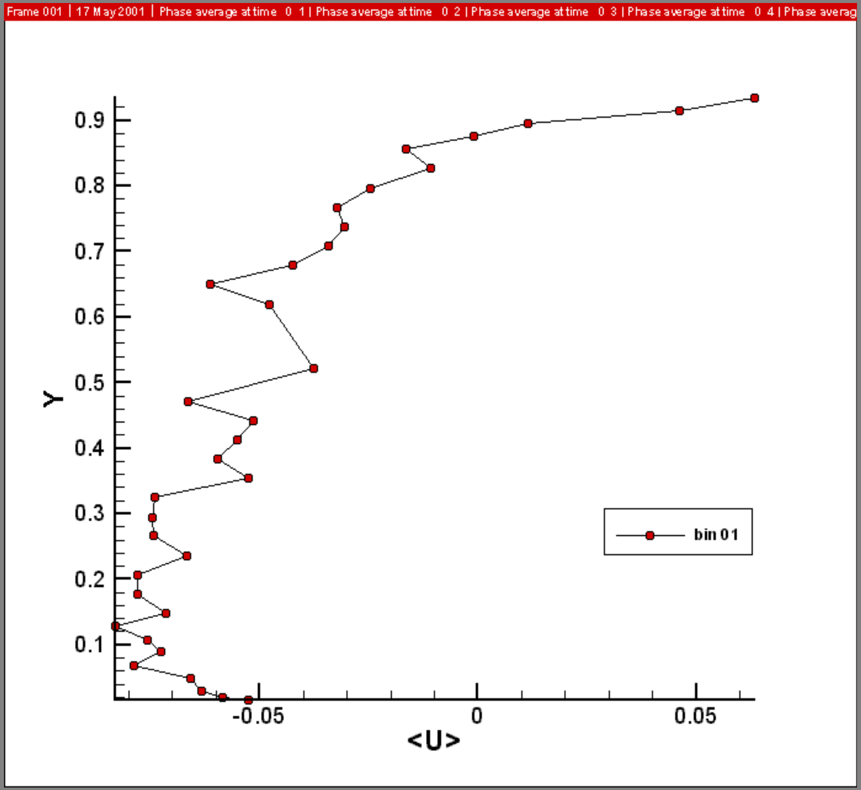

Distribution of random fluctuating components in vertical plane

(a) Horizontal components

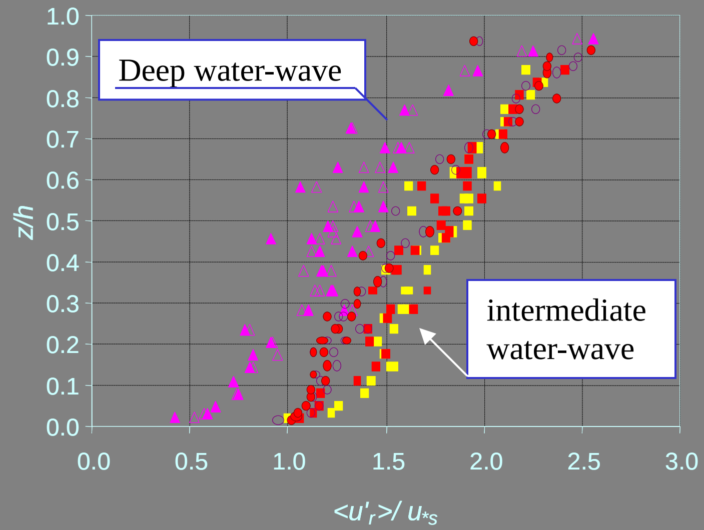

(b) Vertical components

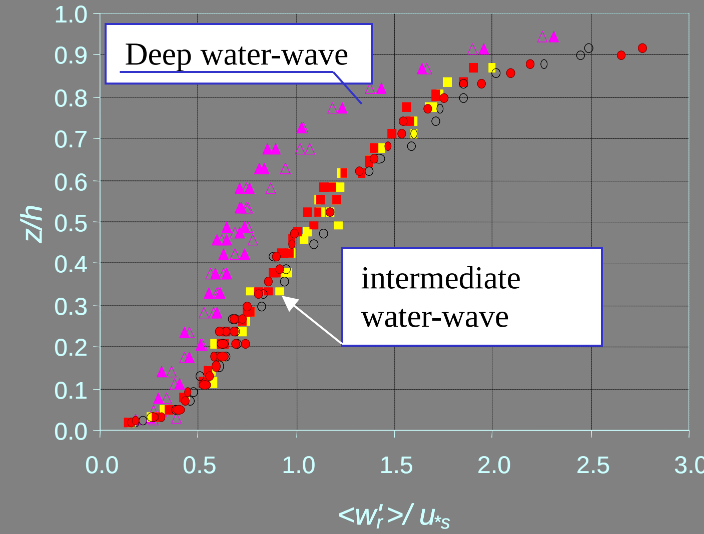

Vector plot in a period for u_g=6.39 m/s and h=63.5 mm (deep water wave conditions)

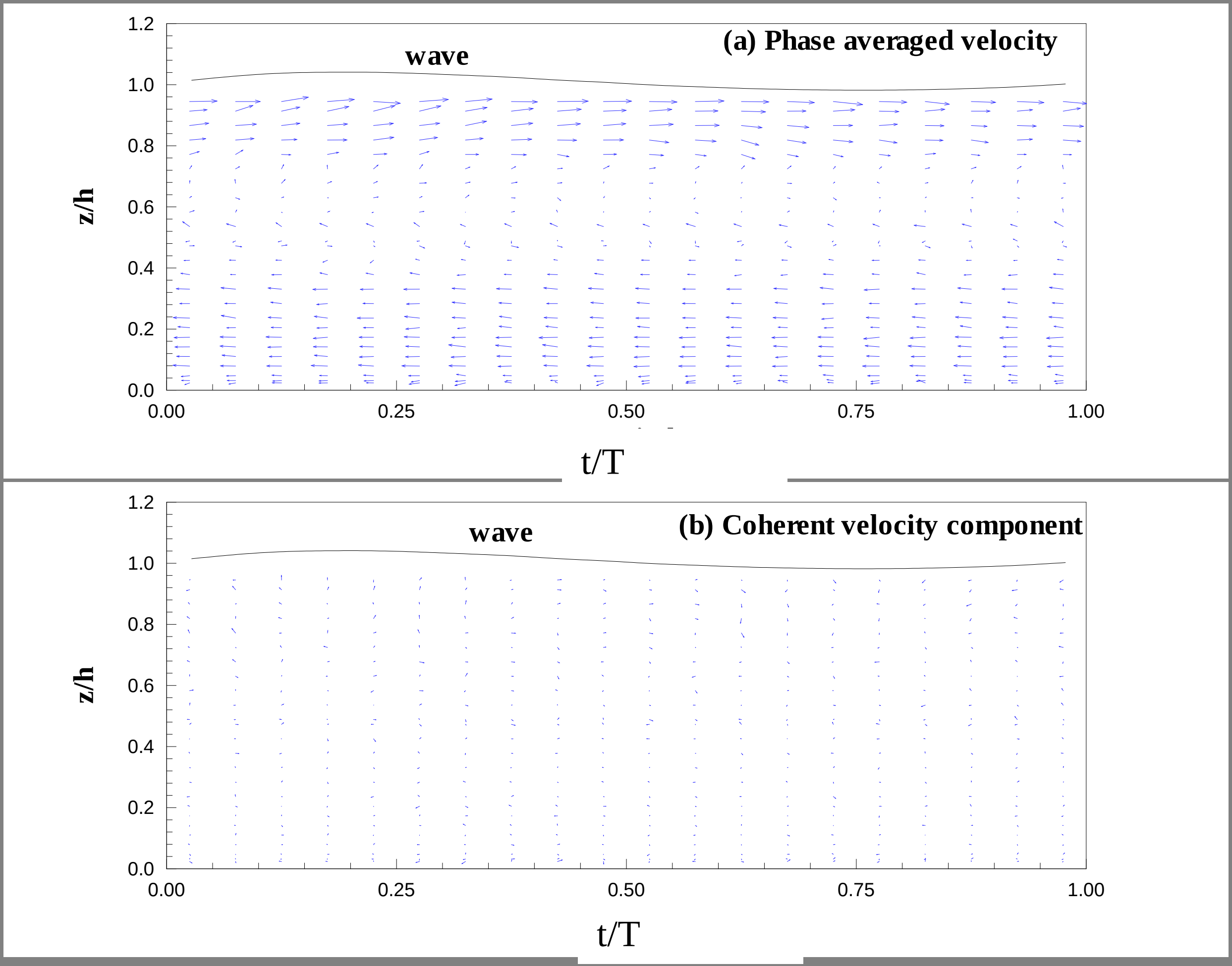

Vector plot in a period for u_g=15 m/s and h=101.6 mm (intermediate water wave condition)

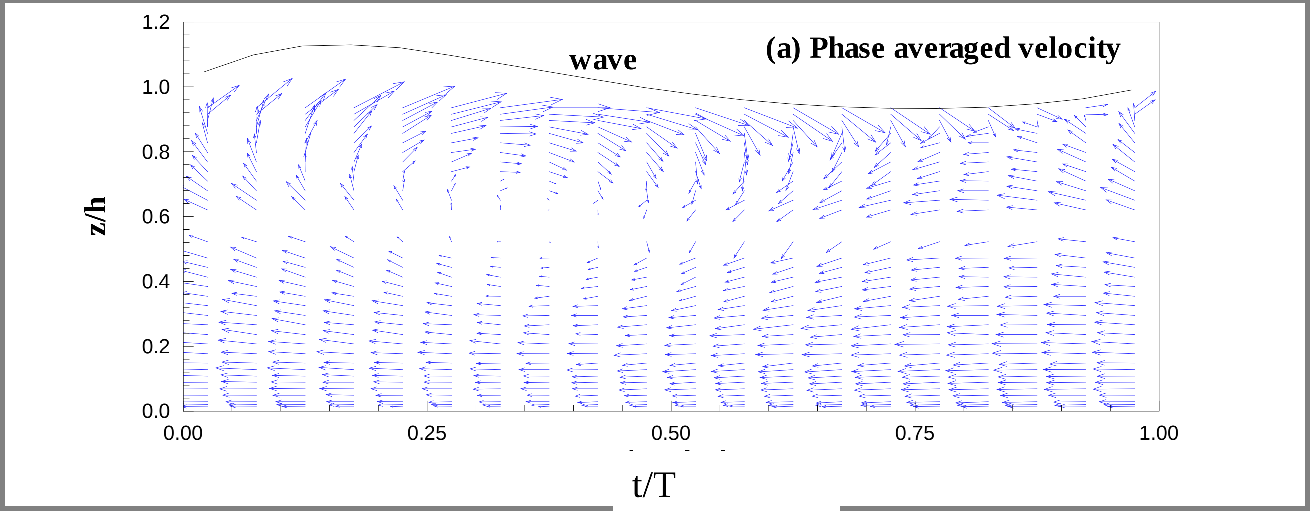

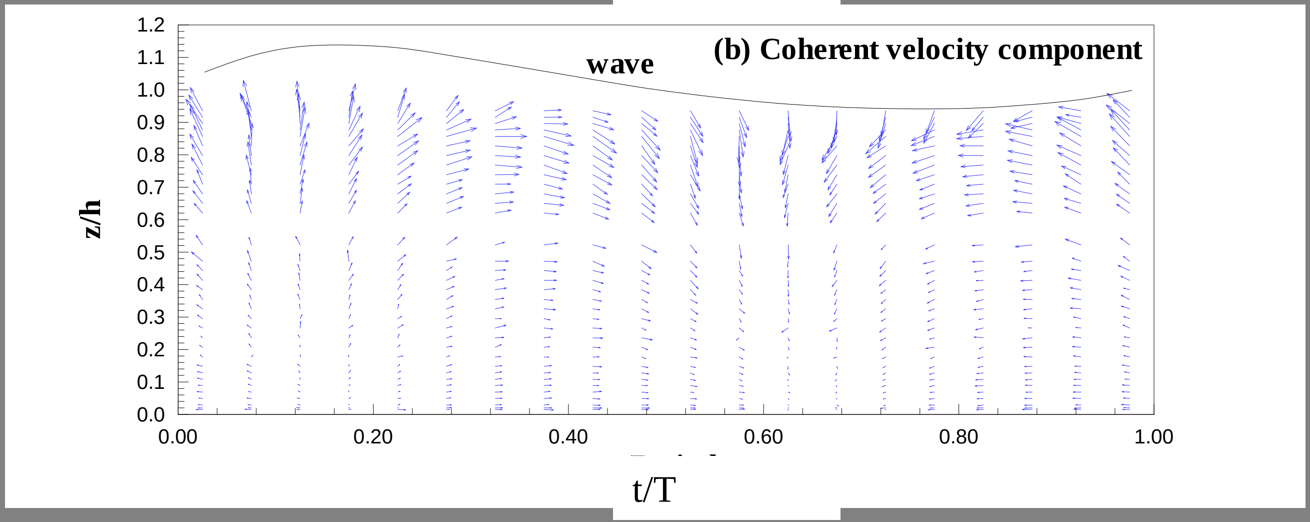

Vector and streamline plot in one wavelength for wind speed u_g=15 m/s and water depth h=101.6 mm (intermediate water wave condition)

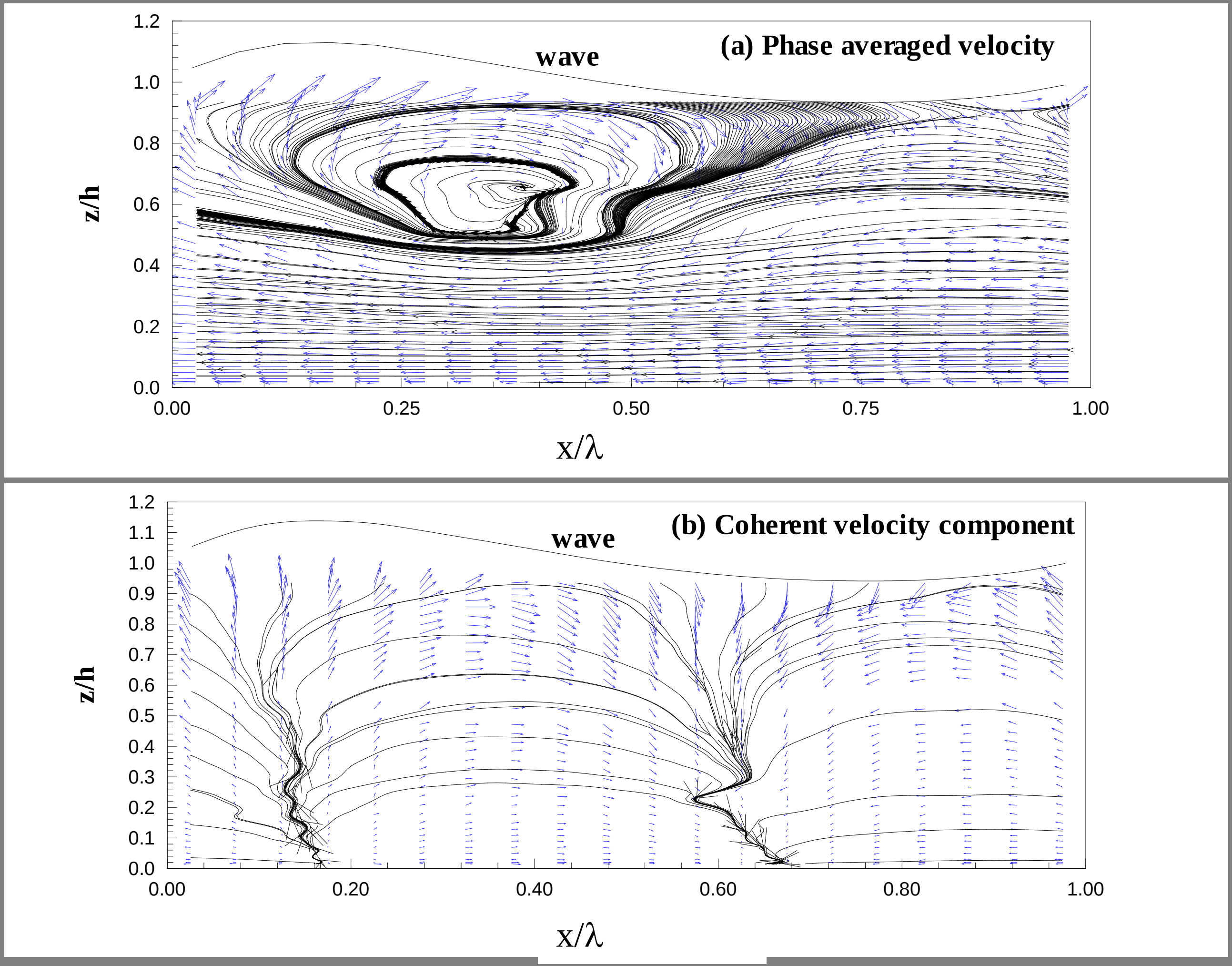

Mathematical modeling

- Time-averaged components
- Coherent components

$$\langle u(z,t)\rangle = \bar{u}(z) + u_c(z,t)$$
$$\langle w(z,t)\rangle = w_c(z,t)$$

Modeling of time-averaged component

Governing equations

$$\frac{\partial \overline{w}}{\partial z} = 0$$

$$-\frac{1}{\rho}\frac{\partial}{\partial x}p + \frac{\partial}{\partial z}\left(\nu_{eff}\frac{\partial \overline{u}}{\partial z}\right) = 0$$

$$-\frac{1}{\rho}\frac{\partial p}{\partial z} = 0$$

Where: $\nu_{eff} = \nu + \nu_t$

Boundary conditions

$z=h$: $u=u_s$ or $\tau=\rho u_{*s}{}^2$

$z=0$: $u=0$

Constrain for countercurrent flow

$$\int_0^h \overline{u}dz = 0$$

Modification of eddy viscosity

Tsanis suggested eddy viscosity (1989):

$$\nu_t = \frac{\lambda u_{*s}}{h}(z + z_b)(z_s + h - z)$$

Proposed eddy viscosity

$$\nu_t = \frac{\lambda u_{*s}}{h}(z + z_b)(z_s + h - z)\left(1 + a\frac{z}{h}\right)$$

Proposed Model of *time-averaged* velocity

$$\frac{\bar{u}}{u_{*s}} = A\ln\left(1+\frac{z}{z_b}\right) + B\ln\left(1-\frac{z}{z_s+h}\right) + C\ln\left(1+a\frac{z}{h}\right)$$

$$A = \frac{(1+a)\ln(1+a) - az_{sh}\ln\left(1+\frac{1}{z_{sh}}\right)}{D}$$

$$B = \frac{(1+a)\ln(1+a) - a(1+z_{bh})\ln\left(1+\frac{1}{z_{bh}}\right)}{D}$$

$$C = \frac{a(1+z_{bh})\ln\left(1+\frac{z}{z_{bh}}\right) - az_{sh}\ln\left(1+\frac{1}{z_{sh}}\right)}{D}$$

$$\begin{aligned} D = \lambda\Big\{ & a\left[1+a(1+z_{sh})\right](1+z_{bh})^2\ln\left(1+\frac{1}{z_{bh}}\right) + \\ & az_{sh}^2(1-z_{bh})\ln\left(1+\frac{1}{z_{sh}}\right) - \\ & (1+z_{bh}+z_{sh})(1+a)^2\ln(1+a)\Big\} \end{aligned}$$

Comparison btwn proposed-model predicted and experimental *time-averaged u* components

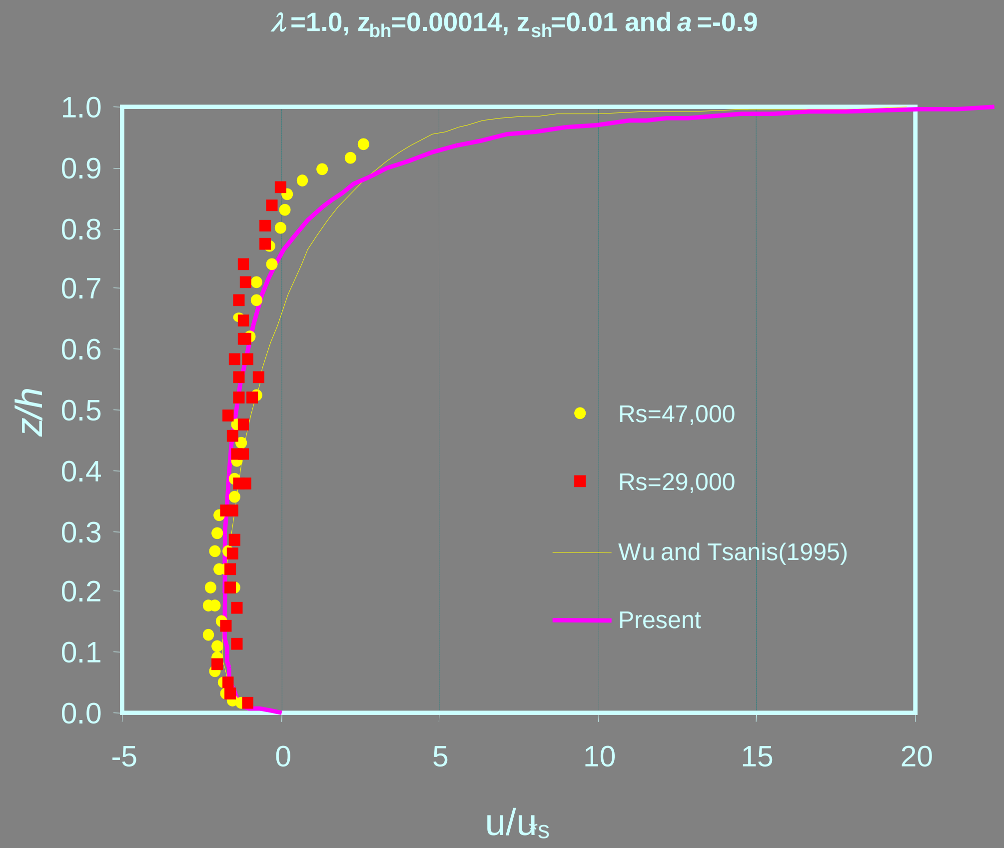

Modeling of *coherent* components

The water particle orbital velocity in a wave can be obtained from the potential flow assumption (i.e. Sorensen, 1993):

$$u(x,z,t) = \frac{\pi H}{T}\frac{\cosh(kz)}{\sinh(kh)}\cos(kx-\sigma t)$$

$$w(x,z,t) = \frac{\pi H}{T}\frac{\sinh(kz)}{\sinh(kh)}\sin(kx-\sigma t)$$

Comparison of model predicted and experimental *coherent* components

Uppermost point

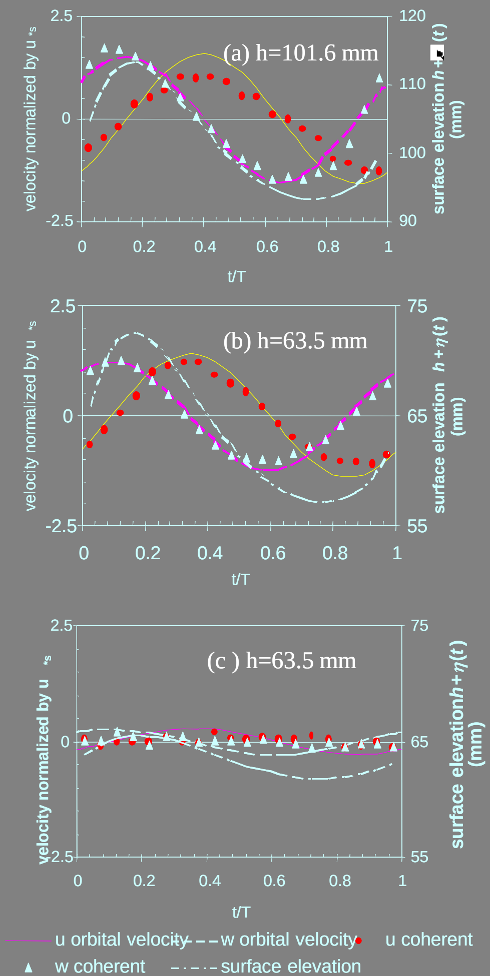

Intermediate water wave

Deep-water wave

Vertical distribution

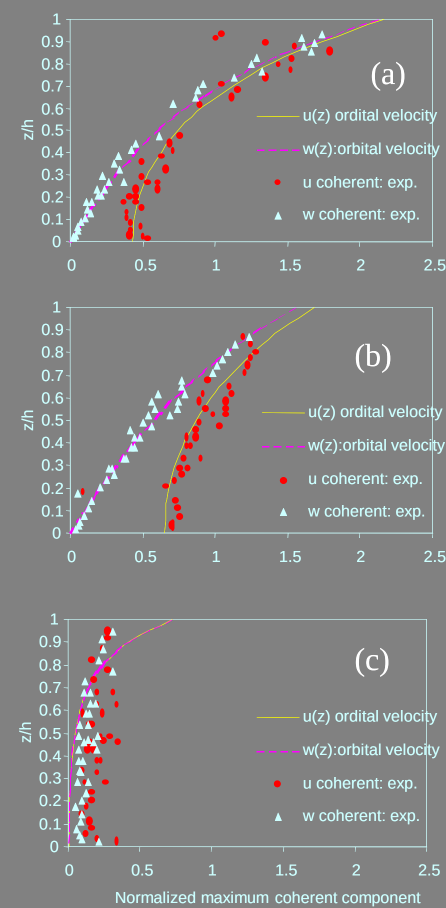

Intermediate water wave

Deep-water wave

Proposed general model for wind-induced countercurrent flow

$$\left\langle \frac{u(x,z,t)}{u_{*s}} \right\rangle = \underbrace{\underbrace{A \ln\left[1+\frac{z}{z_b}\right] + B\ln\left[1-\frac{z}{z_s+h}\right]}_{\text{due to surface shear}} + \underbrace{C\ln\left(1+a\frac{z}{h}\right)}_{\text{due to waves}}}_{\text{time averaged term}} + \underbrace{\frac{\pi H}{T u_{*s}}\left[\frac{\cosh(kz)}{\sinh(kh)}\right]\cos(kx-\sigma t)}_{\text{coherent velocity term}} \qquad 0 \le z \le h$$

$$\left\langle \frac{w(x,z,t)}{u_{*z}} \right\rangle = \underbrace{\frac{\pi H}{T u_{*s}}\left[\frac{\sinh(kz)}{\sinh(kh)}\right]\sin(kx-\sigma t)}_{\text{coherent velocity term}} \qquad 0 \le z \le h$$

Comparison of experimental and model predicted *phase-averaged* velocity <*u*>

(a) Intermediate water wave
$h/\lambda=0.369$, h=101.6 mm

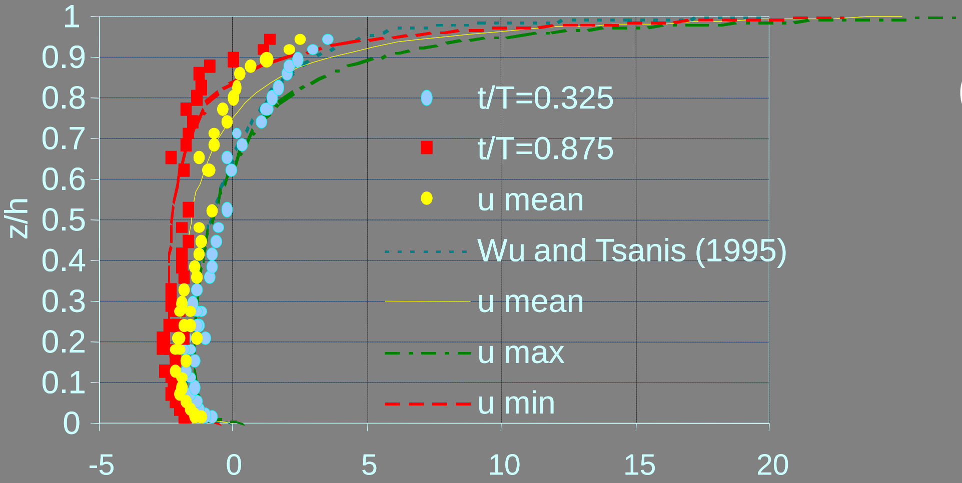

(b) intermediate water wave
$h/\lambda=0.258$, h=63.5 mm

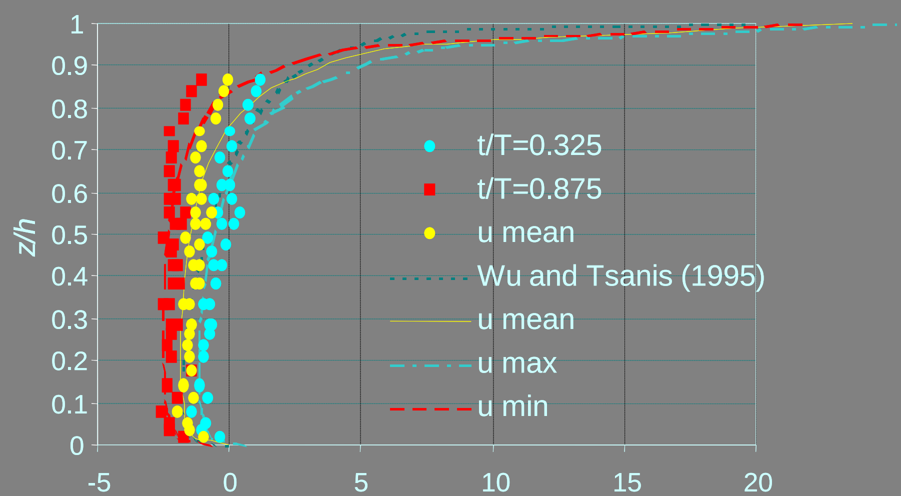

(c) Deep water wave
$h/\lambda=0.866$, h=63.5 mm

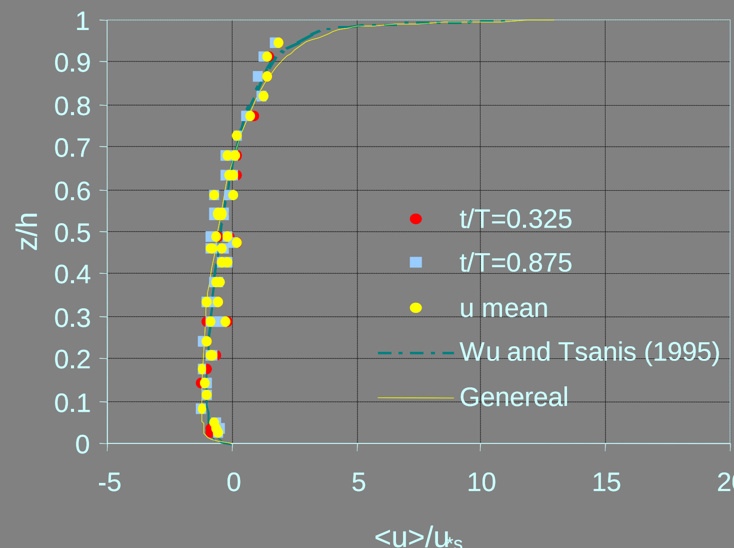

Proposed-model predicted and experimental bed shear stress

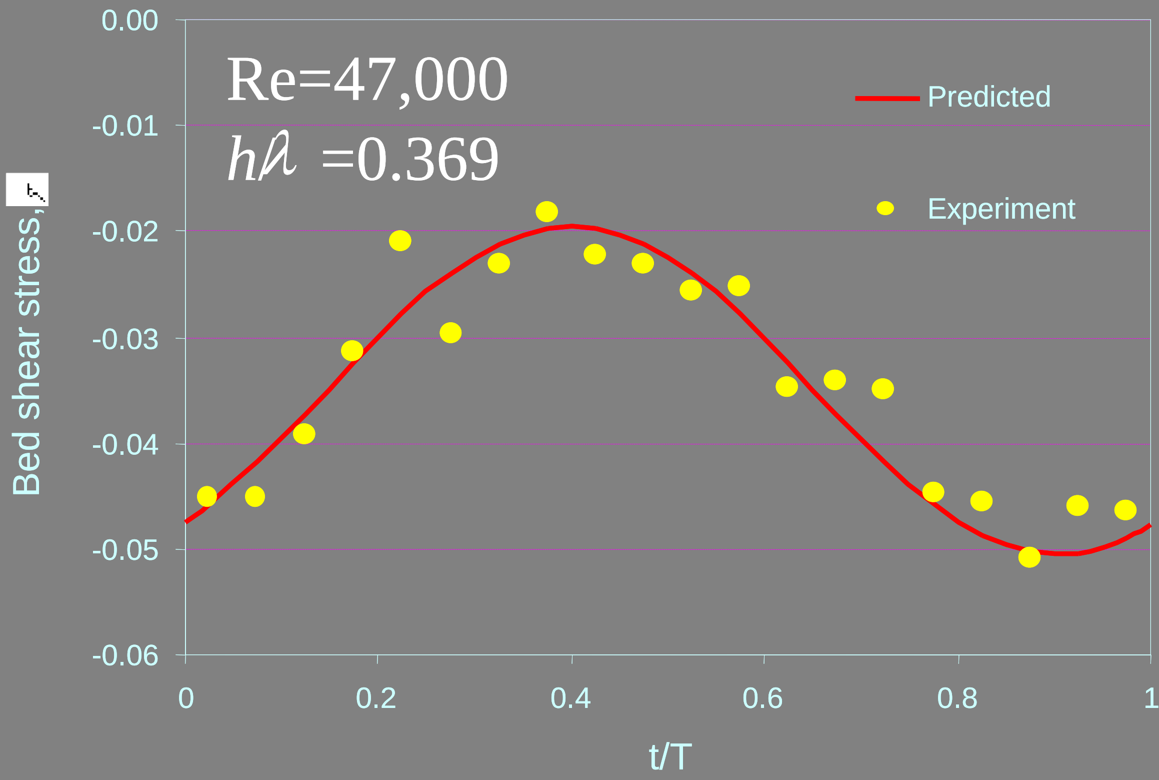

Summary and Conclusions

- The influence of wind-generated water-waves on the flow field is significant under intermediate water-wave conditions, in both the time-averaged and coherent structures of the flow.
- The coherent velocity is closely correlated with surface waves and satisfies linear wave theory, which varies periodically at the frequency of surface waves.
- An organized vortex structure is found in the upper parts of water under intermediate water-waves conditions, which rotates clockwise and travels at the speed of surface waves in the direction of the wind.

Summary and Conclusions (continue)

- The model developed to describe the velocity components is seen to be in excellent agreement with the experimental data and can recover the results of Tsanis (1989) and Wu and Tsanis (1995) for deep-water wave condition.
- The bed shear stress is found to vary periodically with the surface wave frequency under intermediate water waves. Thus, the time-averaged shear stress is not sufficient to quantify the total shear stress.